



HAL
open science

Combinatorial Genetic Modeling of pfcr-t-Mediated Drug Resistance Evolution in Plasmodium falciparum

Stanislaw J Gabryszewski, Charin Modchang, Lise Musset, Thanat Chookajorn, David Fidock

► **To cite this version:**

Stanislaw J Gabryszewski, Charin Modchang, Lise Musset, Thanat Chookajorn, David Fidock. Combinatorial Genetic Modeling of pfcr-t-Mediated Drug Resistance Evolution in Plasmodium falciparum. *Molecular Biology and Evolution*, 2016, 33 (6), pp.1554-1570. 10.1093/molbev/msw037. hal-02862965

HAL Id: hal-02862965

<https://hal.science/hal-02862965>

Submitted on 9 Jun 2020

HAL is a multi-disciplinary open access archive for the deposit and dissemination of scientific research documents, whether they are published or not. The documents may come from teaching and research institutions in France or abroad, or from public or private research centers.

L'archive ouverte pluridisciplinaire **HAL**, est destinée au dépôt et à la diffusion de documents scientifiques de niveau recherche, publiés ou non, émanant des établissements d'enseignement et de recherche français ou étrangers, des laboratoires publics ou privés.

Combinatorial Genetic Modeling of *pfprt*-Mediated Drug Resistance Evolution in *Plasmodium falciparum*

Stanislaw J. Gabryszewski,¹ Charin Modchang,² Lise Musset,³ Thanat Chookajorn,⁴ and David A. Fidock^{*,1,5}

¹Department of Microbiology and Immunology, Columbia University Medical Center, New York

²Department of Physics, Faculty of Science, Mahidol University, Bangkok, Thailand

³Laboratoire de Parasitologie, WHO Collaborating Center for Surveillance of Anti-Malarial Drug Resistance, Institut Pasteur de la Guyane, Cayenne, French Guiana

⁴Genomics and Evolutionary Medicine Unit, Center of Excellence in Malaria, Faculty of Tropical Medicine, Mahidol University, Bangkok, Thailand

⁵Division of Infectious Diseases, Department of Medicine, Columbia University Medical Center, New York, NY

*Corresponding author: E-mail: df2260@columbia.edu.

Associate editor: Csaba Pal

Abstract

The emergence of drug resistance continuously threatens global control of infectious diseases, including malaria caused by the protozoan parasite *Plasmodium falciparum*. A critical parasite determinant is the *P. falciparum* chloroquine resistance transporter (PfCRT), the primary mediator of chloroquine (CQ) resistance (CQR), and a pleiotropic modulator of susceptibility to several first-line artemisinin-based combination therapy partner drugs. Aside from the validated CQR molecular marker K76T, *P. falciparum* parasites have acquired at least three additional *pfprt* mutations, whose contributions to resistance and fitness have been heretofore unclear. Focusing on the quadruple-mutant Ecuadorian PfCRT haplotype Ecu1110 (K76T/A220S/N326D/I356L), we genetically modified the *pfprt* locus of isogenic, asexual blood stage *P. falciparum* parasites using zinc-finger nucleases, producing all possible combinations of intermediate *pfprt* alleles. Our analysis included the related quintuple-mutant PfCRT haplotype 7G8 (Ecu1110 + C72S) that is widespread throughout South America and the Western Pacific. Drug susceptibilities and in vitro growth profiles of our combinatorial *pfprt*-modified parasites were used to simulate the mutational trajectories accessible to parasites as they evolved CQR. Our results uncover unique contributions to parasite drug resistance and growth for mutations beyond K76T and predict critical roles for the CQ metabolite monodesethyl-CQ and the related quinoline-type drug amodiaquine in driving mutant *pfprt* evolution. Modeling outputs further highlight the influence of parasite proliferation rates alongside gains in drug resistance in dictating successful trajectories. Our findings suggest that *P. falciparum* parasites have navigated constrained *pfprt* adaptive landscapes by means of probabilistically rare mutational bursts that led to the infrequent emergence of *pfprt* alleles in the field.

Key words: *Plasmodium falciparum* malaria, drug resistance, evolutionary genetics, transfection, chloroquine, *pfprt* chloroquine resistance transporter.

Introduction

Drug resistance in *Plasmodium* parasites continuously threatens global efforts to control malaria, a leading infectious cause of human morbidity and mortality. Malarial disease is caused by asexual intraerythrocytic protozoan parasites belonging to the genus *Plasmodium*, with life-threatening cases largely attributed to infection with *Plasmodium falciparum* (White et al. 2014). Among the most critical parasite determinants of existing and emerging antimalarial drug resistance is the *P. falciparum* chloroquine resistance transporter (PfCRT), a 424-peptide transmembrane protein with putative involvement in nutrient transport and osmotic balance across the parasite digestive vacuole (DV) membrane (Roepe 2011; Ecker et al. 2012). Fittingly named for its direct role in conferring resistance to the quinoline-type drug chloroquine

(CQ), as validated through genetic linkage (Su et al. 1997) and allelic exchange (Fidock et al. 2000) studies, PfCRT has gained recognition as a multidrug resistance transporter with pleiotropic effects on parasite susceptibility to multiple first-line antimalarials (Ecker et al. 2012; Park et al. 2012; Petersen et al. 2015).

Coinciding with the demise of the short-lived Malaria Eradication Program, the arrival of CQ resistance (CQR) heralded a dramatic increase in severe malaria cases (Trape 2001). A significant association between CQR and *pfprt* was observed in microsatellite typing studies of parasites isolated during this period, which detected four distinct geographical origins of CQR, namely Southeast Asia (with subsequent spread into Africa), the Western Pacific, and two foci in South America (Wootton et al. 2002). Factors that likely

© The Author 2016. Published by Oxford University Press on behalf of the Society for Molecular Biology and Evolution.

This is an Open Access article distributed under the terms of the Creative Commons Attribution Non-Commercial License (<http://creativecommons.org/licenses/by-nc/4.0/>), which permits non-commercial re-use, distribution, and reproduction in any medium, provided the original work is properly cited. For commercial re-use, please contact journals.permissions@oup.com

Open Access

sustained subtherapeutic levels of CQ in the population and thus facilitated the evolution of CQ-resistant *pfprt* alleles include aggressive deployment of CQ as a monotherapy and unregulated use of prophylactic chloroquinated salts (Payne 1988). Despite the setback of resistance to the eradication campaign, CQ played a monumental role in reducing the global burden of malaria (Wellems 2002). CQ continues to be employed for the treatment of uncomplicated *P. falciparum* malaria in regions with no or low-level CQR (Okech et al. 2015) as well as to treat infection with the related malarial parasite *Plasmodium vivax* (Amaratunga et al. 2014).

Mechanistically, CQ interacts with host hemoglobin-derived heme in the DV, where it inhibits detoxification of heme species that are otherwise toxic to parasites (Combrinck et al. 2013). Mutant PfCRT facilitates CQR by reducing the ability of CQ to access its heme target (Fitch 2004; Roepe 2009). This is accomplished by mutant PfCRT-mediated CQ efflux out of the DV and may be further attributed to modulation of PfCRT native function (Roepe 2011; Ecker et al. 2012; Summers et al. 2012). Chemical and molecular features shared among clinically employed antimalarials, including constituents of the first-line artemisinin-based combination therapies (ACTs), collectively include the presence of a CQ-like structural scaffold, accumulation of drug in the DV, inhibition of heme detoxification, and/or drug activation via heme (Hawley et al. 1998; Eastman and Fidock 2009). Consistent with their ability to alter DV physiology, *pfprt* alleles modulate susceptibility to the first-line ACTs and are selected either for or against depending on the specific drug regimen (Ecker et al. 2012). This is underscored by a recent meta-analysis of the clinical efficacy of two widely employed ACTs, artesunate-amodiaquine (AS-AQ) and artemether-lumefantrine (ATM-LUM), which revealed a reduction in time to reinfection for parasites encoding mutant PfCRT in patients treated with AS-AQ, and vice versa for ATM-LUM (Venkatesan et al. 2014). Monitoring resistance to ACT partner drugs is paramount due to the very short half-lives of artemisinins, which leave their long-acting partner drugs solely responsible for clearing any remaining parasites (White 2008). Intriguingly, in vitro and field studies indicate that *pfprt* mutations may even modulate parasites' susceptibility to artemisinins themselves (Sidhu et al. 2002; Henriques et al. 2014; Miotto et al. 2015).

Molecular and epidemiological investigations of the effect of drug pressure on the *pfprt* locus have historically centered on a single-nucleotide polymorphism (SNP) encoding a lysine-to-threonine substitution (K76T) that is highly prevalent among CQ-resistant parasites (Ecker et al. 2012). In parasites expressing CQ-resistant *pfprt* alleles, targeted genetic reversion of PfCRT K76T back to the wild-type residue abolished CQR and its characteristic reversibility by the calcium channel blocker verapamil (VP), in part by enhancing access of CQ to its heme target (Lakshmanan et al. 2005). In line with these in vitro findings, K76T has been associated with in vivo CQR and has served as a sensitive, although not highly specific, marker of CQ treatment failure (Djimde et al. 2001; Goswami et al. 2014), in part due to pre-existing host immunity in areas with high transmission (Djimde et al. 2003).

Mutant *pfprt*-mediated CQR can also be augmented by secondary factors, including mutant *pfmdr1* (Sa et al. 2009; Patel et al. 2010). Of note, geographically distinct CQ-resistant isolates consistently harbor at least three PfCRT mutations in addition to K76T (Ecker et al. 2012; Summers et al. 2012; Baro et al. 2013). These have been conventionally described as compensatory mutations that arose to preserve the essential function of PfCRT (Waller et al. 2003), although their precise contributions to parasite drug resistance and fitness have not been defined.

Antimalarial drugs exert selective pressures on multiple facets of the parasite life cycle, which collectively determine parasite fitness (Mackinnon and Marsh 2010; Rosenthal 2013). Among these are growth of intraerythrocytic parasites, mosquito transmissibility, and within-host virulence, each of which is influenced by the parasite's *pfprt* genotype (Ord et al. 2007; Ecker et al. 2011; Mharakurwa et al. 2013; Lewis et al. 2014; Tukwasibwe et al. 2014; Petersen et al. 2015). A notable example is the mutational status of PfCRT residues 72–76 and its association with the outcome of CQ cessation programs in regions with high-level CQR. In regions in Africa (Mwai et al. 2009; Laufer et al. 2010; Mekonnen et al. 2014) and Asia (Wang et al. 2005; Chen et al. 2008), where the CVIET PfCRT haplotype (residues 72–76) predominates among CQ-resistant parasites, removal of CQ pressure promoted regional resurgences of CQ-sensitive parasites encoding the fitter, wild-type (CVMNK) PfCRT haplotype. In contrast, in South America (Vieira et al. 2004; Gama et al. 2009; Griffing et al. 2010; Adhin et al. 2013) and in select regions elsewhere (de Almeida et al. 2009; Mallick et al. 2012; Khattak et al. 2013; Tan et al. 2014), the predominant mutant PfCRT haplotype, SVMNT, persists despite a decline in CQ use. The prospect that this haplotype is less deleterious to parasites than CVIET (Sa and Twu 2010) is supported by recent in vitro studies, in which isogenic intraerythrocytic parasites expressing the CVIET-encoding Dd2 *pfprt* allele demonstrated a higher fitness cost than parasites expressing the SVMNT-encoding 7G8 *pfprt* allele (Petersen et al. 2015). Accordingly, as they acquire drug resistance-conferring mutations, parasites traverse discrete adaptive landscapes, defined as an organism's fitness as a function of the mutational events incurred (Olson-Manning et al. 2012). The ability to ascertain evolutionary histories of *pfprt* alleles and identify predictable mutational pathways would be of particular relevance to region-specific treatment recommendations, which are routinely informed by *pfprt* genotypes.

To date, the adaptive landscapes of drug resistance alleles consisting of n mutations have been explored through rigorous combinatorial approaches, in which an experimental proxy for fitness is determined for all 2^n possible mutational intermediates and used to quantify the accessibility of the $n!$ possible stepwise evolutionary trajectories leading to the full-length resistance allele (Poelwijk et al. 2007; Hartl 2014). Subsequent comparison of accessible trajectories can illuminate preferred mutational pathways and uncover epistatic interactions between mutant residues that may constrain the evolutionary potential of a gene of interest (Weinreich et al. 2006; Kogenaru et al. 2009). For *Plasmodium*, such combinatorial analyses have not previously been performed for

PfCRT and have been limited to heterologous expression studies that explored the mutational acquisition of dihydrofolate reductase-mediated antifolate resistance (Lozovsky et al. 2009; Brown et al. 2010; Costanzo et al. 2011; Jiang et al. 2013).

The feasibility of mapping mutational trajectories accessible to *P. falciparum* parasites is greatly facilitated by recent advances in genome editing strategies (de Koning-Ward et al. 2015). In this study, we utilized *pfcr*t-specific zinc finger nucleases (ZFNs) to conduct a combinatorial genetic dissection of the CQ-resistant South American *pfcr*t allele Ecu1110 during the pathogenically relevant parasite asexual blood stage. Consisting of the fewest number of mutations observed in a CQ-resistant parasite, the Ecu1110 PfCRT haplotype (K76T, A220S, N326D, I356L) is closely related to the highly prevalent 7G8 haplotype, which differs by the presence of a single additional mutation (C72S). Here, we profiled the drug susceptibility and in vitro growth of isogenic parasites expressing all possible *pfcr*t alleles spanning the evolutionary transition from CQ-sensitive (wild-type) to CQ-resistant (Ecu1110), as well as the CQ-resistant *pfcr*t allele 7G8. These experimentally derived genotype–phenotype relationships were subsequently applied to an evolutionary model in order to probe the adaptive landscape of parasites as they acquire drug resistance. This is the first combinatorial description of the trade-offs experienced by *P. falciparum* parasites as they acquire mutations in the *pfcr*t gene, a core determinant of antimalarial drug resistance.

Results

Generation of a Combinatorial Panel of *pfcr*t Alleles in Isogenic *Plasmodium falciparum* Parasites

Surveys of PfCRT haplotypes in geographically distinct CQ-resistant isolates of *P. falciparum* indicate that CQR requires at least four mutations, namely K76T and at least three accompanying nonsynonymous mutations (Ecker et al. 2012). Although this suggests that CQ-resistant parasites necessitate compensatory mutations to maintain PfCRT function, several key questions remain unanswered: Which SNPs directly influence drug resistance, which neutralize fitness costs, and which contribute in both regards? Are there predictable mutational trajectories in the evolution of PfCRT-mediated drug resistance? To address these questions, our study centered on the CQ-resistant Ecuadorian *pfcr*t allele Ecu1110 (Fidock et al. 2000), which harbors four mutations and is therefore amenable to a comprehensive dissection of the genetic determinants of parasite drug resistance and fitness.

To perform a combinatorial analysis of *pfcr*t, we used ZFNs (supplementary fig. S1, Supplementary Material online) to genetically engineer a series of intraerythrocytic parasites encoding all 16 combinations of the 4 mutations that comprise the Ecu1110 allele. These are K76T, A220S, N326D, and I356L, which we respectively refer to as Ecu_A, Ecu_B, Ecu_C, and Ecu_D, with the quadruple-SNP Ecu1110 haplotype represented as Ecu_{ABCD} (table 1). Due to the slow growth of the Ecu1110 parasite strain in culture, we introduced the full set

Table 1. Summary of PfCRT Haplotypes.^a

PfCRT haplotype	PfCRT Residue				
	72	76	220	326	356
GC03 (wild-type)	C	K	A	N	I
Ecu _A	C	T	A	N	I
Ecu _B	C	K	S	N	I
Ecu _C	C	K	A	D	I
Ecu _D	C	K	A	N	L
Ecu _{AB}	C	T	S	N	I
Ecu _{AC}	C	T	A	D	I
Ecu _{AD}	C	T	A	N	L
Ecu _{BC}	C	K	S	D	I
Ecu _{BD}	C	K	S	N	L
Ecu _{CD}	C	K	A	D	L
Ecu _{ABC}	C	T	S	D	I
Ecu _{ABD}	C	T	S	N	L
Ecu _{ACD}	C	T	A	D	L
Ecu _{BCD}	C	K	S	D	L
Ecu1110 (Ecu _{ABCD})	C	T	S	D	L
7G8	S	T	S	D	L

^aMutations different from the GC03 (wild-type) PfCRT haplotype are indicated in gray. DNA substitutions encoding each PfCRT mutation are as follows: C72S: TGT→AGT; K76T: AAA→ACA; A220S: GCC→TCC; N326D: AAC→GAC; I356L: ATA→TTA.

of combinatorial alleles into the South American recipient strain 7G8. This line is derived from a Brazilian clinical isolate (Burkot et al. 1984) and has been successfully used to modify the *pfcr*t locus in recent ZFN-based studies (Pelleau et al. 2015). The highly prevalent, quintuple-SNP 7G8 PfCRT haplotype is distinguished from Ecu1110 PfCRT by one additional mutation (C72S; table 1) and was included in our allelic panel. This parasite line, 7G8^{7G8} (recombinant *pfcr*t allele indicated in superscript), served as a control for ZFN-based modification of *pfcr*t and was comparable with genetically unedited 7G8 parasites with regard to CQ susceptibility and growth rates.

Our ZFN-based genetic engineering strategy is depicted in supplementary figure. S1A, Supplementary Material online. Briefly, we constructed a donor plasmid for each combinatorial *pfcr*t allele (table 1), which was transfected into 7G8 recipient parasites. Donor plasmid-enriched parasites were subsequently transfected with a plasmid encoding *pfcr*t-specific ZFNs that were previously validated (Straimer et al. 2012). Homology-directed repair of DNA breaks catalyzed by these ZFNs yielded the recombinant *pfcr*t locus (supplementary fig. S1B, Supplementary Material online). For each recombinant line, two individual clones were isolated for subsequent analysis. Genetic editing of the *pfcr*t locus was evaluated by diagnostic polymerase chain reactions (supplementary fig. S1C, Supplementary Material online), followed by sequencing of parasite genomic DNA and cDNA using primers listed in supplementary table S1, Supplementary Material online. Additionally, *pfcr*t sequence integrity was monitored in all recombinant parasite lines throughout the duration of all assays. Phenotypic differences between parasite strains were not attributable to levels of PfCRT expression (supplementary table S2, Supplementary Material online).

Effect of *pfcr* Combinatorial Alleles on Parasite CQ Susceptibility

To evaluate the contribution of PfCRT SNPs to parasite resistance to CQ and its primary active metabolite, monodesethyl-CQ (md-CQ), we subjected our panel of *pfcr*-modified (table 1) isogenic parasite lines to flow cytometry-based drug susceptibility assays and determined drug inhibitory concentrations that cause 50% (IC₅₀) and 90% (IC₉₀) inhibition of parasite growth. We also analyzed the genetically unmodified reference lines GC03, Ecu1110, and 7G8 (corresponding PfCRT haplotypes listed in table 1). Antimalarial IC₅₀ and IC₉₀ values are summarized in supplementary tables S3 and S4, Supplementary Material online, respectively. For all strains tested, drug responses were compared against those of isogenic 7G8^{GC03} parasites, which encode the wild-type (GC03) *pfcr* allele (table 1).

Our drug susceptibility findings for CQ (fig. 1A) and md-CQ (fig. 1B) revealed that the CQR-associated mutation K76T is insufficient for parasite CQR. Intriguingly, as compared with 7G8^{GC03} parasites, 7G8^{EcuA} parasites exhibited significant md-CQ hypersensitivity (mean IC₅₀ values of 20.9 and 15.1 nM, respectively; supplementary table S3, Supplementary Material online), highlighting a critical role for mutations beyond K76T in conferring CQR. This is further corroborated by the md-CQ responses of multiple lines with PfCRT haplotypes lacking K76T (7G8^{EcuC}, 7G8^{EcuD}, 7G8^{EcuBC}, 7G8^{EcuCD}, 7G8^{EcuBCD}), which showed modest (1.5- to 2.5-fold) yet significant elevations in md-CQ IC₅₀ as compared with 7G8^{GC03} parasites (fig. 1B and supplementary table S3, Supplementary Material online). The reduced md-CQ susceptibility of these lines was accentuated at the IC₉₀ level (supplementary table S4, Supplementary Material online).

To dissect the impact of specific SNPs on parasite drug resistance, we compared the drug responses of PfCRT haplotype pairs differing at only one residue. For every combinatorial PfCRT haplotype, we determined the successive contribution of each Ecu1110 PfCRT-specific SNP to CQ and md-CQ resistance (supplementary table S5, Supplementary Material online). We considered all instances in which mutational acquisition conferred a significant change in CQ or md-CQ IC₅₀ as compared with the precursor PfCRT haplotype. Invariably, in all such instances, Ecu_C N326D served to increase drug resistance. Ecu_D I356L similarly conferred increased drug resistance, with one exception (Ecu_C→Ecu_{CD}; supplementary table S5, Supplementary Material online), whereby it decreased md-CQ resistance. In contrast, Ecu_B A220S only increased resistance in the context of triple-SNP PfCRT haplotypes, while conferring decreased md-CQ resistance for double-SNP haplotypes. The mutational milieu was likewise important for Ecu_A K76T, which decreased drug resistance for haplotypes leading up to the triple-SNP stage, at which point it conferred increased resistance. In addition, as compared with Ecu_{ABCD}, we observed significantly increased CQ (fig. 1A; $P < 0.001$) and md-CQ (fig. 1B; $P < 0.01$) IC₅₀ values for 7G8 PfCRT, indicating a direct role for C72S, the sole distinction between these two haplotypes (table 1).

A characteristic trait of in vitro parasite CQR is its reversibility by VP, which was previously linked to the parasite *pfcr* locus via quantitative trait loci mapping (Patel et al. 2010). To examine the roles of specific *pfcr* mutations on VP reversibility of CQR, we assessed parasite susceptibility to CQ in the presence or absence of 0.8 μM VP and computed the CQ response modification index (RMI), defined as the ratio between the IC₅₀ for CQ plus VP and the IC₅₀ for CQ alone (fig. 1C and supplementary table S6, Supplementary Material online). Consistent with published VP reversibility profiles (Sa et al. 2009), Ecu1110 and 7G8 reference parasites exhibited comparable VP chemosensitization of CQR (1.5- to 1.9-fold reductions in CQ RMI relative to the CQ-sensitive line GC03). This finding was recapitulated by isogenic parasites expressing the corresponding *pfcr* alleles (1.7- to 1.8-fold reductions in CQ RMI for 7G8^{EcuABCD} and 7G8^{7G8} relative to 7G8^{GC03}). Moreover, we noted direct roles for K76T and N326D in the VP reversibility effect, as the mutational acquisition of Ecu_A K76T by the Ecu_{BCD} PfCRT haplotype and the acquisition of Ecu_C N326D by the Ecu_{ABD} haplotype both conferred VP-reversible CQR to parasites encoding the resulting Ecu_{ABCD} haplotype ($P < 0.01$ for both trajectories).

Effect of *pfcr* Combinatorial Alleles on Parasite Susceptibility to ACT Component Drugs

In view of the role of PfCRT as a determinant of parasite multidrug resistance (Ecker et al. 2012), we investigated the influence of combinatorial PfCRT haplotypes on parasite susceptibility to the artemisinin compound AS and the ACT partner drugs AQ and LUM (fig. 2 and supplementary tables S3 and S4, Supplementary Material online), which comprise the widely used ACT formulations AS-AQ and ATM-LUM (Eastman and Fidock 2009). The quinoline-type antimalarial AQ is of particular interest due to its historical use in regions with parasites harboring the Ecu1110 and 7G8 *pfcr* alleles (Sa and Twu 2010). Focusing on the clinically relevant metabolite of AQ, monodesethyl-AQ (md-AQ), we observed substantial overlap between parasites' susceptibility to md-AQ (fig. 2A and supplementary table S3, Supplementary Material online) and md-CQ (fig. 1B and supplementary table S3, Supplementary Material online). This is consistent with cross-resistance between CQ and AQ that is mediated in part by PfCRT variants (Ecker et al. 2012). Similar to our results for CQ, K76T was insufficient to confer md-AQ resistance (fig. 2A and supplementary table S3, Supplementary Material online). Of note, an important role in mediating md-AQ resistance was uncovered for Ecu_C N326D, as acquisition of N326D by any PfCRT haplotype lacking this mutation consistently conferred elevated md-AQ IC₅₀ and/or IC₉₀ values (supplementary tables S3 and S4, Supplementary Material online). As 7G8^{7G8} parasites showed significantly higher md-AQ IC₅₀ values than 7G8^{EcuABCD} parasites ($P < 0.01$), we also identified a contributory role for PfCRT C72S in md-AQ resistance.

Treatment of parasite lines with the arylaminoalcohol drug LUM yielded more subtle differences in drug response (fig. 2B and supplementary table S3, Supplementary

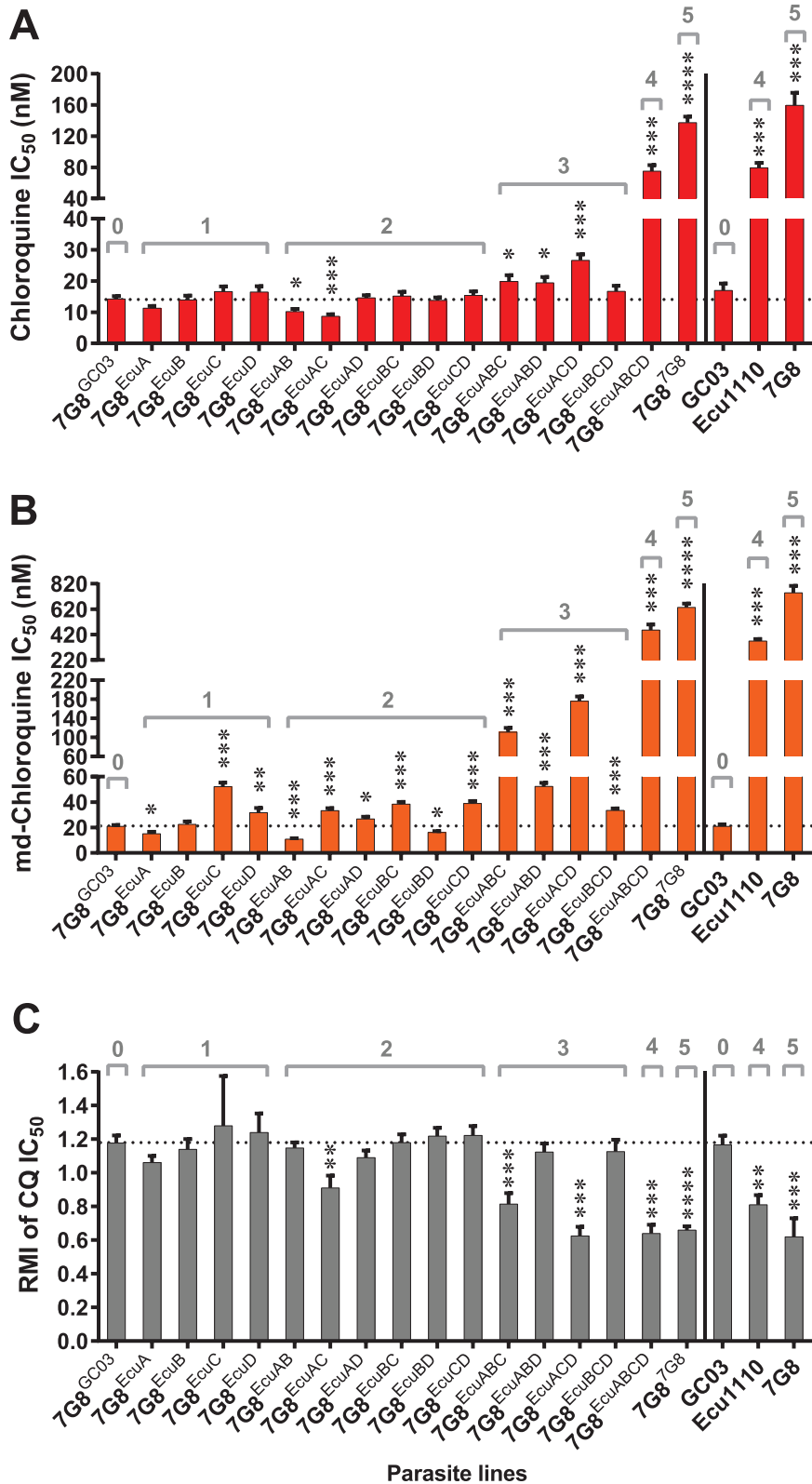


Fig. 1. CQ resistance profiles of *pfCRT*-modified and reference parasite lines. Parasite growth inhibition was determined by flow cytometry after 72 h exposure to serial dilutions of (A) CQ, (B) md-CQ, or (C) CQ in the presence or absence of 0.8 μ M VP. Bar graphs represent (A, B) mean \pm SEM IC₅₀ values or (C) mean \pm SEM CQ RMI values, equivalent to (IC₅₀ for CQ + VP)/(IC₅₀ for CQ only). Results encompass 5–15 independent assays conducted in duplicate. Statistical differences were determined via nonparametric Mann–Whitney *U* tests, using the mean IC₅₀ value of wild-type *pfCRT*-expressing 7G8^{GC03} parasites (dotted black line) as the comparator. The total number of *pfCRT* mutations encoded by parasite lines is indicated in gray. When applicable, the y-axis was split to illustrate subtle, statistically significant differences in IC₅₀ values. IC₅₀, IC₉₀, and CQ RMI values are summarized along with corresponding statistical tests in [supplementary tables S3, S4, and table S6, Supplementary Material online](#), respectively. **P* < 0.05; ***P* < 0.01; ****P* < 0.001. *****P* < 0.0001.

Material online). Compared with the 7G8^{GC03} line, we observed a modest (1.4-fold), although significant, increase in LUM susceptibility for 7G8^{7G8} parasites, in line with previous reports that CQ-resistant PfCRT haplotypes confer increased LUM susceptibility (Sisowath et al. 2009). We attribute the constricted range of observed LUM IC₅₀ values to the high sensitivity of the 7G8 genetic background to LUM at baseline (Petersen et al. 2015). Our LUM susceptibility findings nevertheless illustrate that *pfprt* mutations exert opposing forces on parasite LUM resistance (e.g., 7G8^{EcuABC} and 7G8^{EcuD}, respectively, showed elevated and reduced LUM IC₅₀ values, as compared with 7G8^{GC03}; fig. 2B and supplementary table S3, Supplementary Material online).

Consistent with previous in vitro investigations (Sidhu et al. 2002), our collection of combinatorial *pfprt* alleles modulated parasite susceptibility to the artemisinin compound AS (fig. 2C and supplementary table S3, Supplementary Material online). As anticipated, full-length mutant *pfprt* alleles significantly increased AS sensitivity (1.5- to 1.7-fold decrease in AS IC₅₀ for 7G8^{EcuABCD} and 7G8^{7G8} as compared with 7G8^{GC03}). Interestingly, K76T was sufficient to confer increased parasite AS sensitivity (1.6-fold decrease in AS IC₅₀ for 7G8^{EcuA} vs. 7G8^{GC03}). Additionally, increased parasite AS resistance was afforded upon acquisition of Ecu_D I356L, with two distinct mutational trajectories (Ecu_{AB}→Ecu_{ABD} and Ecu_{AC}→Ecu_{ACD}; fig. 2C and supplementary table S3, Supplementary Material online) conferring significant elevations in AS IC₅₀ values ($P < 0.01$ and $P < 0.05$, respectively).

Effect of *pfprt* Combinatorial Alleles on In Vitro Parasite Growth

As organisms acquire mutations in response to drug pressure, they experience fitness constraints that affect the course of their adaptive evolution. Accordingly, we evaluated the impact of our set of combinatorial *pfprt* alleles on the in vitro growth of intraerythrocytic parasites, which serves as a proxy for fitness (Hartl 2014; Hughes and Andersson 2015). To initiate the growth assays, we seeded cocultures with equal (1:1) proportions of CQ-sensitive (wild-type *pfprt*) green fluorescent protein (GFP)-positive (GFP⁺) reporter parasites and *pfprt*-modified GFP-negative (GFP⁻) test parasites. Cocultures were established in the absence or presence of a sublethal dose of CQ (7.5 nM; $0.5 \times$ CQ IC₅₀ of CQ-sensitive reporter line). Using flow cytometry, we regularly determined the proportion of coculture expressing the test *pfprt* allele (GFP⁻ parasite population). The relative proportions of parasite populations were recorded every third day for ten generations (supplementary fig. S2A, Supplementary Material online), natural log-transformed (supplementary fig. S2B, Supplementary Material online), and subjected to a linear regression analysis (Hartl 2014; Petersen et al. 2015). To quantify parasite fitness costs, we derived the relative fitness (ω') of a given parasite line as compared with isogenic, wild-type *pfprt*-expressing parasites (7G8^{GC03}) in the absence of drug pressure and computed the per-generation selection coefficient (s) for each line as per the relationship $s = \omega' - 1$. Thus, as compared with the wild-type *pfprt* allele, $s = 0$, $s > 0$, and s

< 0 signify alleles that are selectively neutral, advantageous, and disadvantageous, respectively.

As compared with the 7G8^{GC03} parasite line, our isogenic, *pfprt*-modified parasites exhibited various degrees of in vitro fitness (range of mean s values: -0.26 to 0.11), with the majority of *pfprt* alleles conferring comparable ($s = 0$) or inferior ($s < 0$) relative fitness (fig. 3 and supplementary table S7, Supplementary Material online). A notable exception was the Ecu_{AD} haplotype, which demonstrated significantly enhanced relative fitness ($s = 0.07$ – 0.11 , i.e., 7–11% growth advantage per parasite generation). Although we did not observe a selective advantage for any *pfprt* alleles in the presence of 7.5 nM CQ, this subtherapeutic CQ concentration had a significantly deleterious impact on the growth of parasites encoding haplotypes Ecu_A, Ecu_C and Ecu_{AB} (fig. 3 and supplementary table S7, Supplementary Material online). Notably, in this genetic background, PfCRT K76T was insufficient for CQR and had a deleterious impact on parasite growth that was exacerbated by CQ. Interestingly, expression of the full-length Ecu1110 PfCRT haplotype in the Ecu1110 genetic background was associated with a significant reduction in growth as compared with the 7G8 background (14% per-generation growth disadvantage for Ecu1110 vs. 7G8^{Ecu1110} parasites, regardless of CQ pressure; $P < 0.0001$). This suggests the presence of additional fitness-enhancing genetic factors in the 7G8 genetic background.

We further examined the specific contribution of PfCRT SNPs to in vitro parasite growth by identifying all instances in which mutational acquisition conferred a significant change in growth as compared with the precursor PfCRT haplotype (supplementary table S8, Supplementary Material online). In all such cases, K76T, A220S, and N326D (Ecu_A, Ecu_B, and Ecu_C, respectively) had a deleterious impact on parasite growth, with a single exception for Ecu_A K76T (increased growth for Ecu_D→Ecu_{AD}; supplementary table S8, Supplementary Material online). In contrast, Ecu_D I356L consistently increased in vitro growth. Additionally, as compared with Ecu_{ABCD}, 7G8 PfCRT conferred enhanced in vitro growth (10% growth advantage per generation for 7G8^{7G8} vs. 7G8^{EcuABCD} parasites, regardless of CQ pressure; $P < 0.0001$). Thus, in this genetic background, the 7G8 hallmark mutation C72S (table 1) positively contributed to both parasite drug resistance and growth rate.

Modeling the Evolution of *pfprt*-Mediated CQR

The course of *P. falciparum* drug resistance evolution is shaped by the adaptive landscapes parasites traverse as they acquire drug resistance mutations. To further explore *pfprt* adaptive landscapes, we employed a modified computational model based on previously established algorithms (Lozovsky et al. 2009; Brown et al. 2010; Kumpornsin et al. 2014), as detailed in Materials and Methods. Briefly, experimentally derived drug resistance and growth data for isogenic parasites encoding all *pfprt* alleles spanning the transition from CQ-sensitive (wild-type; GC03) to CQ-resistant (Ecu1110) were used to simulate adaptive landscapes, and the mutational pathway accessibility was subsequently determined for each landscape. Pathways were deemed accessible

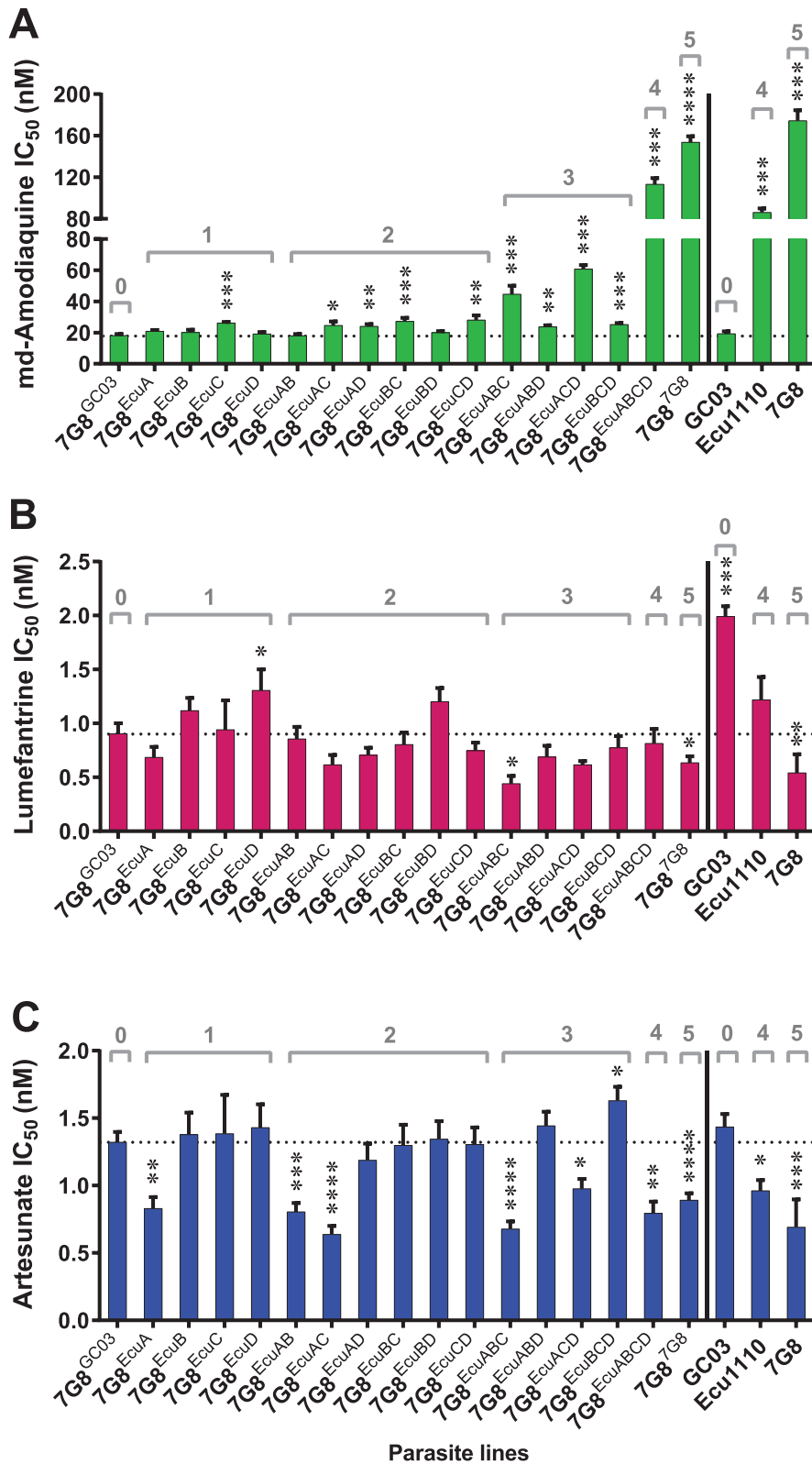


Fig. 2. Susceptibility of *pfprt*-modified and reference parasite lines to first-line antimalarial compounds md-AQ, LUM, and AS. Parasite growth inhibition was determined by flow cytometry after 72 h exposure to serial dilutions of (A) md-AQ, (B) LUM, or (C) AS. Bar graphs indicate mean IC₅₀ values ± SEM, as determined in 4–17 independent assays conducted in duplicate. Statistical differences were determined via nonparametric Mann–Whitney *U* tests, using the mean IC₅₀ value of wild-type *pfprt*-expressing 7G8^{GC03} parasites (dotted black line) as the comparator. The total number of *pfprt* mutations encoded by parasite lines is indicated in gray. When applicable, the y-axis was split to illustrate subtle, statistically significant differences in IC₅₀ values. IC₅₀ and IC₉₀ values, numbers of assays, and corresponding statistical tests are summarized in [supplementary tables S3 and S4, Supplementary Material online](#). **P* < 0.05; ***P* < 0.01; ****P* < 0.001. *****P* < 0.0001.

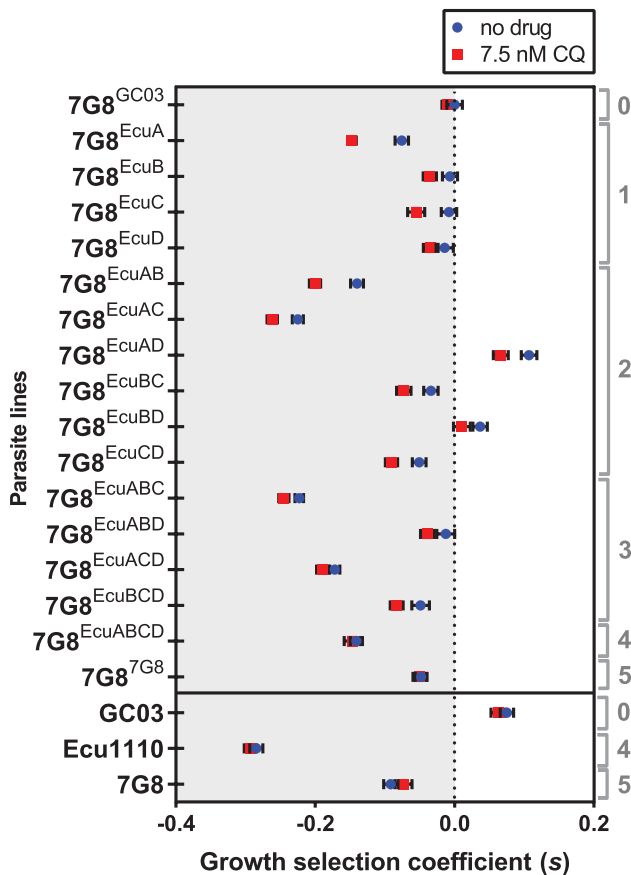


Fig. 3. In vitro growth of *pfprt*-modified and reference parasite lines. To assess parasite in vitro growth, cocultures initially consisting of a 1:1 ratio of a single GFP⁻ test (recombinant or reference) line and a GFP⁺ reporter line (R^{GFP}) were monitored by flow cytometry for ten generations. Three independent assays were conducted in duplicate in the absence or presence of a sublethal dose of CQ (7.5 nM, equivalent to $0.5 \times$ CQ IC₅₀ of CQ-sensitive R^{GFP} line). The per-generation selection coefficient (*s*) for each test strain was derived from parasite growth curves (supplementary fig. S2, Supplementary Material online), as detailed in Materials and Methods. Shown are mean \pm SEM *s* values for lines subjected to no drug or 7.5 nM CQ. The total number of *pfprt* mutations encoded by parasite lines is indicated in gray. Mean *s* values as well as results of interstrain and intrastrain statistical tests are summarized in supplementary table S7, Supplementary Material online.

only if each mutational step led to a progressive increase in the total fitness (f_T) of parasites. In our evolutionary model, f_T is composed of normalized parasite growth (f_G) and drug resistance (f_D) indices as per the relationship $f_T = af_D + (1-a)f_G$, where f_D represents normalized IC₅₀ values, f_G represents normalized relative in vitro growth values (ω') in the absence of drug, and the drug pressure coefficient a represents drug inhibitory level. In our simulations, f_D and f_G indices were generated from normal distributions based on the means and standard error of the means (SEMs) of *pfprt* allele-specific IC₅₀ and ω' values, respectively. Our model considers the role of drug pressure in facilitating CQR evolution via the drug pressure coefficient a (range 0–1). Thus, selection is based solely on parasite growth rates for $a = 0$ and on parasite drug resistance for $a = 1$. Inspection of the parasite

growth index (f_G) plotted as a function of the drug resistance index (f_D) based on simulations performed for CQ and md-CQ (fig. 4) revealed comparable trade-off profiles for the parent drug and its active metabolite, with no significant correlation observed between f_G and f_D , as per Pearson's correlation analysis (CQ: $R^2 = 0.057$, $P = 0.37$; md-CQ: $R^2 = 0.15$, $P = 0.13$).

Evolutionary modeling was first performed to determine the realization probabilities for the mutational pathways (p) leading from wild-type to the full-length Ecu1110 *pfprt* allele via sequential acquisition of single mutations (0→1→2→3→4; fig. 5A). Modeling was performed for a range of drug pressure scenarios by varying the coefficient a from 0 to 1 in 0.1 increments. For every a value, each of 10^4 adaptive landscapes was subjected to 10^5 evolutionary excursions (10^9 total excursions), and mutational pathway realization probabilities were recorded for modeling based on CQ (fig. 5B) and md-CQ (fig. 5C) data. The i^{th} pathway absolute realization probability (P_i) was calculated from the formula N_i/N_{total} , where N_i is the number of times that the simulations achieve the Ecu_{ABCD} allele by traversing pathway i , and N_{total} is the total number of runs (see Materials and Methods). Pathway realization probabilities for evolutionary modeling of CQ and md-CQ resistance are reported in supplementary tables S9 and S10, Supplementary Material online, respectively. For both drugs, p20 (fig. 5A) showed the maximum realization probability, with a >10-fold increase in predictive ability for the active metabolite as compared with the parent drug (9.43×10^{-7} for CQ vs 1.39×10^{-5} for md-CQ). Highlighting the important interaction between parasite resistance (f_D) and growth (f_G) in dictating drug resistance evolution, the highest realization probabilities in both cases occurred for simulations in which total parasite fitness (f_T) was informed by both f_D and f_G indices ($a = 0.8$).

Based on total pathway realization probabilities for both CQ and md-CQ modeling, the top two Ecu1110 *pfprt* evolutionary pathways were p20 and p19 (supplementary tables S9 and S10, Supplementary Material online), which feature Ecu_D I356L as the first mutation acquired (fig. 5A). Remarkably, although accessible trajectories were observed for both pathways for a wide range of drug pressure scenarios (supplementary fig. S3, Supplementary Material online), many excursions through these pathways were inaccessible due to the existence of adaptive valleys (i.e., f_T not progressively increasing), as highlighted by plots of mean f_T values encompassing all adaptive landscapes generated in our analysis for both CQ (fig. 5D) and md-CQ (fig. 5E) modeling. Our data show that, of the 10^9 total excursions simulated for each a value for the 0→1→2→3→4 mutational scenario, CQ-directed and md-CQ-directed evolution of the full-length Ecu1110 *pfprt* allele was respectively supported by $\leq 9.4 \times 10^2$ and $\leq 1.4 \times 10^4$ excursions, with no appreciable effect on total parasite fitness (f_T) until the three-SNP intermediate (Ecu_{ABD} or Ecu_{ACD}).

In the scenario of CQR evolution via sequential acquisition of single mutations (0→1→2→3→4), three distinct mutational intermediates spanned the transition from wild-type to Ecu1110 *pfprt*. Given the apparent adaptive constraints associated with this evolutionary course, we next explored

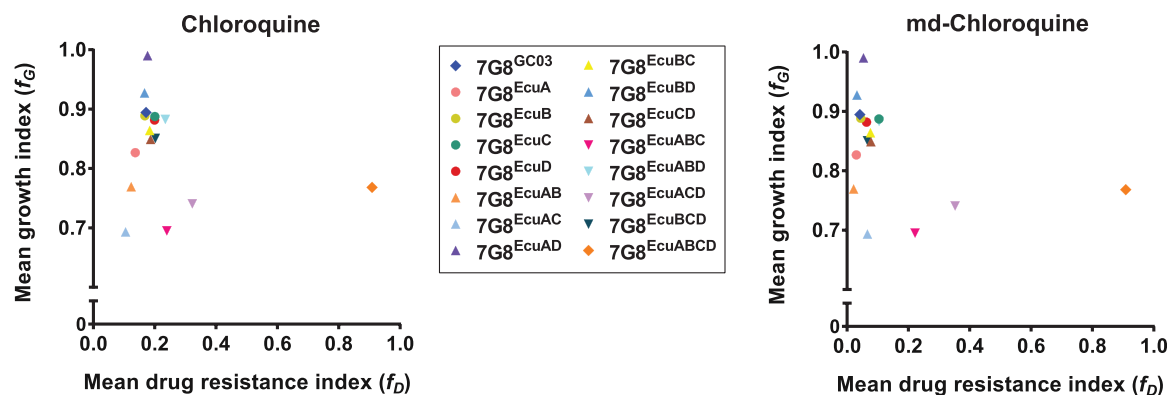


FIG. 4. Trade-offs between parasite in vitro growth and drug resistance. For each *pfcr*-modified strain, relative growth (f_G) in the absence of drug pressure was plotted as a function of the parasite's relative resistance (f_D) to CQ or md-CQ. Calculation of f_G and f_D is detailed in Materials and Methods.

trajectories in which up to three mutations were acquired simultaneously, thus requiring fewer intermediates. These scenarios could occur with pre-existing alleles and/or with pressure from other antimalarials. Evolutionary modeling was performed as for the $0 \rightarrow 1 \rightarrow 2 \rightarrow 3 \rightarrow 4$ mutational scenario, with 10^9 total evolutionary excursions examined for various drug pressure scenarios (range of a values: 0 to 1). Results for CQ and md-CQ mutational pathways requiring either two ($0 \rightarrow 1 \rightarrow 2 \rightarrow 4$; $0 \rightarrow 1 \rightarrow 3 \rightarrow 4$; or $0 \rightarrow 2 \rightarrow 3 \rightarrow 4$) or one ($0 \rightarrow 1 \rightarrow 4$; $0 \rightarrow 2 \rightarrow 4$; or $0 \rightarrow 3 \rightarrow 4$) intermediate steps are illustrated in [supplementary figs. S4 and S5, Supplementary Material online](#), respectively. Pathway probabilities are listed in [supplementary tables S9 and S10, Supplementary Material online](#). Consistent with our results for the $0 \rightarrow 1 \rightarrow 2 \rightarrow 3 \rightarrow 4$ mutational scenario, the top realized pathways overwhelmingly featured initial acquisition of Ecu_D I356L and/or Ecu_C N326D. Notably, for both CQ and md-CQ modeling, mutational sequences $0 \rightarrow 1 \rightarrow 3 \rightarrow 4$ and $0 \rightarrow 3 \rightarrow 4$ yielded realization probabilities up to $\sim 10^5$ -fold greater than those for the $0 \rightarrow 1 \rightarrow 2 \rightarrow 3 \rightarrow 4$ scenario (e.g., compare total probabilities for p1-24 and p71-p74 in [supplementary tables S9 and S10, Supplementary Material online](#)). This suggests the possibility that rare bursts of multiple mutations facilitated the emergence of CQR-conferring *pfcr* alleles.

Modeling of md-AQ-Directed *pfcr* Evolution

Given the known cross-resistance between CQ and AQ and the historical use of AQ in South America, where the $Ecu1110$ and $7G8$ *PfCRT* haplotypes are common (see Discussion), we also explored the impact of AQ drug pressure on $Ecu1110$ *pfcr* evolution. Similar to the CQ and md-CQ evolutionary modeling, we performed evolutionary modeling for md-AQ, the primary active metabolite of AQ. Our results are shown in [supplementary figure S6, Supplementary Material online](#), for a range of mutational scenarios, with pathway probabilities detailed in [supplementary table S11, Supplementary Material online](#). Indicating extensive overlap between CQ and AQ in directing *pfcr* evolution, the majority (77.8%) of top pathways based on md-AQ modeling ([supplementary table S11, Supplementary Material online](#)) coincided with top pathways as identified by md-CQ modeling ([supplementary table S10,](#)

[Supplementary Material online](#)). A role for md-AQ in aiding *pfcr* evolution is further evident from comparisons of total realization probabilities associated with different quinoline-type drugs ([table 2](#)). As compared with CQ and md-CQ, md-AQ-directed *pfcr* evolution yielded, respectively, upwards of >10 -fold and >100 -fold increases in accessibility for the sequential, single-step mutational scenario ($0 \rightarrow 1 \rightarrow 2 \rightarrow 3 \rightarrow 4$; see p23 in [table 2](#)). Similar to CQ and md-CQ, for scenarios in which mutational intermediates were skipped due to simultaneous acquisition of more than one mutation, md-AQ-directed evolution was comparably associated with a substantial increase in pathway accessibility (e.g., compare p23 and p73 in [table 2](#) and compare total probabilities for p1-24 and p71-p74 in [supplementary table S11, Supplementary Material online](#)).

It is noteworthy that the CQR-conferring $7G8$ *pfcr* allele remains the most prevalent allele in South America, despite declines in CQ and AQ use in this region ([Vieira et al. 2004](#); [Sa and Twu 2010](#)). As $7G8$ *pfcr* is distinguished from the $Ecu1110$ *pfcr* allele by the presence of a single additional mutation (C72S; [table 1](#)), our modeling of $Ecu1110$ *pfcr* evolution may be used to draw inferences about the evolution of the highly prevalent $7G8$ allele. Collectively, our data indicate that, in the $7G8$ genetic background, *PfCRT* C72S confers increased parasite resistance to the quinoline compounds CQ, md-CQ, and md-AQ, while simultaneously enhancing parasite growth. Thus, we postulate that the top mutational pathways identified for the evolution of $Ecu1110$ *pfcr* also represent mutational paths leading to the evolution of $7G8$ *pfcr*.

Discussion

In this study, we harnessed ZFN-based combinatorial genetics and computational evolutionary modeling to probe the evolutionary trajectories accessible to parasites as they acquire mutations in the *pfcr* gene, the primary determinant of CQR and a key modulator of susceptibility to several currently deployed antimalarials ([Ecker et al. 2012](#)). Our simulations revealed pronounced biological constraints associated with the evolution of $Ecu1110$ *pfcr*, a prototypical CQ-resistant allele comprised of four mutations, the smallest number required for resistance ([Fidock et al. 2000](#)). Among the

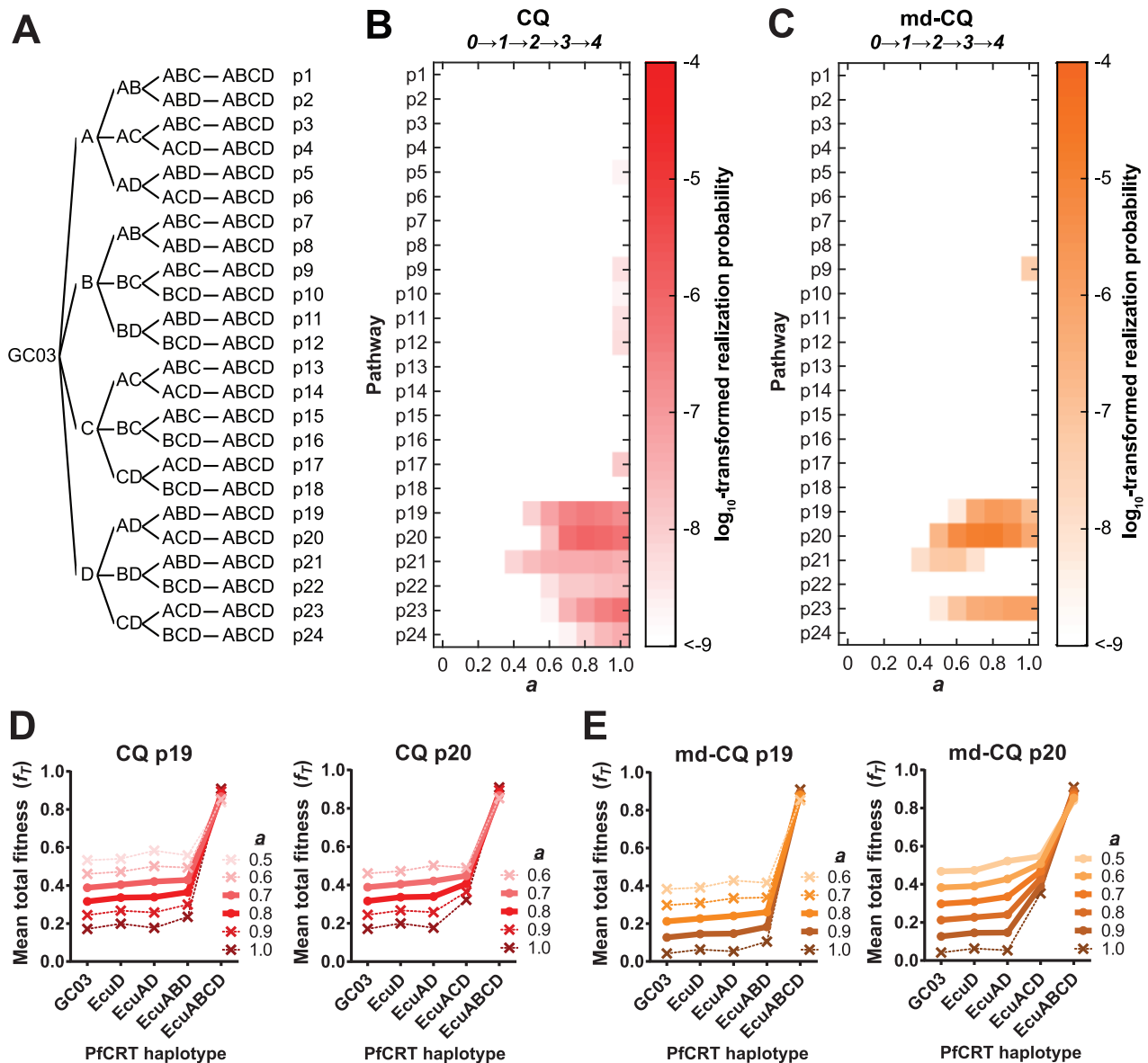


Fig. 5. Modeling of CQ and md-CQ-directed *pfprt* evolution. (A) Schematic of the 24 theoretical pathways (p1–p24) leading from wild-type (GC03) to Ecu1110 (ABCD) PfCRT via the sequential (i.e., 0→1→2→3→4) acquisition of single mutations A, B, C, and D. These correspond to Ecu1110 PfCRT constituent mutations K76T, A220S, N326D, and I356L, respectively. Accessibility of mutational pathways for (B) CQ-directed and (C) md-CQ-directed evolutionary modeling. Briefly, adaptive landscapes were simulated based on experimentally derived parasite drug resistance and growth indices and used to quantify the realization probability for a given mutational pathway (see Materials and Methods). Simulations explored the effect of drug pressure (a), from $a = 0$ (no pressure, i.e., growth rates fully dictate trajectory) to $a = 1$ (full pressure, i.e., parasite resistance fully dictates trajectory). Heat map color intensity corresponds to \log_{10} -transformed pathway realization probability. Adaptive landscapes illustrating the interplay of total parasite fitness (f_T), mutations acquired, and extent of drug pressure (a). With regard to the total realization probability for all a values, the top two realized (D) CQ-directed and (E) md-CQ-directed mutational pathways are p19 and p20. Shown are trajectories for each of these mutational pathways based on mean f_T values, which encompass the complete set of simulated adaptive landscapes for each drug. Accessible (i.e., f_T increases progressively) and inaccessible (i.e., f_T valleys are present) trajectories are indicated by thick lines/circles and dotted lines/crosses, respectively. Plots of representative accessible mutational trajectories are shown in [supplementary figure S3, Supplementary Material online](#).

pathways based on the sequential accumulation of single mutations leading to the Ecu1110 allele, the maximum realization probabilities for CQ and md-CQ resistance were, respectively, $\sim 5 \times 10^{-7}$ and $\sim 10^{-6}$ ([supplementary tables S9 and S10, Supplementary Material online](#)). In comparison, earlier modeling of pyrimethamine resistance evolution mediated by the sequential gain of up to four mutations in the

pfdhfr gene ([supplementary table S12, Supplementary Material online](#)) showed a maximum realization probability of $\sim 3 \times 10^{-4}$ ([Kumpornsin et al. 2014](#)). These findings are consistent with historical records showing that the evolution of drug-resistant forms of *pfprt* in natural parasite populations occurred more rarely than for mutant *pfdhfr* ([Wongsrichanalai et al. 2002](#)).

Table 2. Representative *pfCRT* Mutational Trajectories Accessible to Quinoline Drug Resistance Evolution.^a

Pathway	Mutational intermediates					Total realization probability		
	0	1	2	3	4	CQ	md-CQ	md-AQ
p20	WT	D	AD	ACD	ABCD	2.8×10^{-6}	3.8×10^{-5}	1.1×10^{-4}
p23	WT	D	CD	ACD	ABCD	8.8×10^{-7}	3.2×10^{-6}	1.5×10^{-4}
p47	WT	D	—	ACD	ABCD	2.3×10^{-3}	7.9×10^{-3}	3.9×10^{-3}
p73	WT	—	—	ACD	ABCD	2.3×10^{-1}	5.4×10^{-1}	5.1×10^{-1}

NOTE.—0–4, number of mutations comprising the given *PfCRT* haplotype; —, skipped mutational intermediate; WT, wild type (GC03); D, EcuD; AD, EcuAD; ACD, EcuACD; ABCD, EcuABCD (Ecu1110).

^aTotal realization probabilities for the collectively most accessible mutational pathways (*p*) identified in modeling of CQ, md-CQ, and md-AQ resistance evolution (supplementary tables S9–S11, Supplementary Material online). Shown are the two most accessible pathways for the 0→1→2→3→4 mutational scenario, as well as the most accessible pathways for the 0→1→3→4 and 0→3→4 scenarios. *PfCRT* haplotypes are listed in table 1.

Our modeling of *pfCRT* evolution uncovered multiple adaptive valleys (fig. 5D and E) associated with the sequential acquisition of single mutations, such that the gain of a subsequent mutation generally constrained resistance evolution by reducing the total parasite fitness (f_T). We consequently examined scenarios in which two or more mutations were acquired simultaneously. This analysis revealed pathways with vast increases in accessibility (up to a maximum total realization probability of $\sim 2 \times 10^{-1}$ and $\sim 5 \times 10^{-1}$ for CQ and md-CQ, respectively; supplementary tables S9 and S10, Supplementary Material online). As the fixation of *pfCRT* alleles bearing one to three mutations has not been documented in the field, we hypothesize that *pfCRT*-mediated CQR arose through mutational bursts with brief periods of intervening growth, whereby one or more mutations were acquired and expanded during a short time window prior to the acquisition of additional mutations. Based on our combined IC_{50} and growth data, the most likely scenario would be the near-simultaneous emergence of three to four mutations. Although this would be an exceptionally infrequent event, we note several months of intermittent in vitro pressure of a CQ-resistant *P. falciparum* strain (K1) with the antimalarial halofantrine selected for a *pfCRT* variant with three additional point mutations (Johnson et al. 2004).

Mathematical modeling of the acquisition of multiple mutations in response to selective pressure has previously shown that the temporality of mutational events, population size, and duration of evolution might jointly facilitate the emergence of mutations with a frequency significantly greater than the cumulative product of single-mutation rates, previously estimated to be $\sim 10^{-9}$ for *P. falciparum* (Zheng 2003; Bopp et al. 2013; Claessens et al. 2014). In the absence of evidence for hypermutator *P. falciparum* lineages (Bopp et al. 2013; Brown et al. 2015), the emergence of Ecu1110 *pfCRT* in the low-transmission setting of South America can be attributed to the convergence of multiple factors, including the extent of drug pressure on parasite populations, monoclonality of infections, rate of genetic exchange between strains during sexual stage development in the mosquito vector, and host immunity (Hughes and Andersson 2015). Of note, our model did not specifically investigate mutational reversion and conversion events (Palmer et al. 2015), which could help overcome suboptimal peaks in the *pfCRT* adaptive landscape. Additional *pfCRT* mutations might also have been acquired

via meiotic recombination between intermediate alleles in *P. falciparum* sexual stages.

Our analysis of the Ecu1110 and 7G8 *pfCRT* allelic variants leads us to speculate on the evolution of the Dd2 allele, which carries eight point mutations and dominates in Southeast Asia. This allele, or a similar isoform, earlier spread from Asia into Africa, resulting in the widespread loss of CQ efficacy (Wellems 2004). We postulate that the Dd2 allele occurred via one or more major bursts of multiple mutations in a very limited number of parasites that spread under selective CQ pressure. Resultant population bottlenecks would have consequently diminished the effective population size, reduced competition with fitter wild-type parasites, and enabled mutant parasites to traverse fitness valleys toward high-level resistance (DePristo et al. 2005). We note that the Dd2 allele, while more CQ-resistant than the 7G8 allele, demonstrates a significant fitness cost (Lewis et al. 2014; Petersen et al. 2015). Evidence of ongoing selection is provided by the emergence in Cambodia of the Cam734 *pfCRT* allele that harbors nine mutations (of which five are not found in Dd2) and that, while less CQ-resistant than Dd2, confers a level of parasite fitness comparable with the wild-type allele (Petersen et al. 2015).

Prior combinatorial modeling of *pfDHFR* evolution in yeast has shown that in vitro growth rates can serve as a robust assessment of organismal fitness (Brown et al. 2010). In the absence of a comprehensive way to account for all biological characteristics that impact fitness during the complex *Plasmodium* life cycle, we quantified the parasite growth index (f_C) associated with specific *pfCRT* mutations. Our analysis was performed within the pathogenically relevant setting of asexual blood stage infection, during which parasite numbers can rapidly increase and be exposed to drug pressure. The critical role of the f_C parameter and its interplay with parasite drug resistance (f_D) is demonstrated by the modulation of evolutionary pathway accessibilities by the drug pressure coefficient a , which governed the relative influence of f_C and f_D in dictating *pfCRT* evolution (fig. 5). Our study illuminates mutational determinants of asexual blood stage parasite fitness. Most notably, Ecu_D I356L consistently contributed to enhanced in vitro parasite growth and was the most accessible primary mutational step in our CQ and md-CQ evolutionary excursions. Interestingly, this mutation also increased AS IC_{50} values (fig. 2C), evoking the recent association of the I356T

mutation in Southeast Asia with *k13*-mutant artemisinin-resistant parasite populations (Miotto et al. 2015).

Recent studies with *P. falciparum* parasites differing in their *pfcr* allele have found that CQR-conferring PfCRT isoforms cause the accumulation of high levels of hemoglobin-derived peptides in the parasite DV, which was associated with a deleterious impact on parasite growth (Lewis et al. 2014). Future studies with our combinatorial *pfcr* variants can be used to address the impact of specific mutations on hemoglobin digestion. Given that the evolution of *pfcr*-mediated CQR also required successful transmission of variant PfCRT isoforms to the mosquito vector, examining the effect of specific *pfcr* mutations on transmission is equally merited. This is of interest in light of rodent malaria studies that demonstrated a transmission advantage associated with the expression of the 7G8 *pfcr* allele in CQ-treated gametocytes (Ecker et al. 2011).

Our genetic dissection recalls important insights from recent studies of CQ transport mediated by PfCRT isoforms heterologously expressed in either *X. laevis* or *S. cerevisiae* (Summers et al. 2014; Callaghan et al. 2015). In agreement with both studies, we observed Ecu_A K76T to be insufficient for CQR and uncovered direct contributions to CQR by additional PfCRT mutations, in particular Ecu_C N326D. Crystallographic insights, presently lacking for PfCRT or its homologs, indicate that even seemingly conservative substitutions (e.g., isoleucine to leucine, as in I356L) can significantly impact a protein's structure and function (Wu et al. 2015). In addition to PfCRT I356L, the apparent need for mutational acquisition of basic, polar, and acidic side chains at residues 76, 220, and 326, respectively, suggests specific electrostatic and conformational requirements for PfCRT-mediated CQR. Our findings clarify previous discussions about the role of non-K76T mutations, which have been surmised to solely compensate for a loss of native PfCRT function (Hastings et al. 2002; Cooper et al. 2005; Egan and Kuter 2013). Of note, in vitro and field-based studies have also observed that parasites harboring the conventional CQR marker K76T can acquire novel PfCRT mutations (e.g., C101F or C350R) that abolish resistance to CQ (Eastman et al. 2011; Pelleau et al. 2015), emphasizing the need for caution in interpreting the CQ susceptibility status of isolates based on incomplete *pfcr* genotypes.

Interestingly, as compared with Ecu1110 PfCRT, which lacks the C72S mutation, 7G8 PfCRT conferred decreased rates of CQ transport (Summers et al. 2014; Callaghan et al. 2015), yet increased the degrees of CQR and in vitro growth in *P. falciparum*. It is noteworthy that, in studies of isogenic parasite lines encoding variant PfCRT haplotypes from the Philippines (PH1 and PH2) that likewise only differ at residue 72, C72S conferred increased parasite CQR, yet in that case reduced parasite growth (Petersen et al. 2015). Collectively, these findings underscore the impact of the overall mutational milieu on the roles of specific *pfcr* mutations. Furthermore, they raise the prospect that certain mutations may alleviate CQ-mediated inhibition of native PfCRT function without having a direct impact on drug transport.

In selecting the geographically related 7G8 parasite genetic background (Burkot et al. 1984) for our combinatorial analysis, we aimed to single out the specific contributions of and interactions between *pfcr* mutations in the evolution of the quintuple-SNP 7G8 *pfcr* allele that is widespread throughout South America. Of note, we did not observe desired allelic replacement events in our initial efforts to engineer *pfcr* alleles (namely Ecu_A and Ecu_{ABCD}) in GC03 (CQ-sensitive) parasites, which were derived from an earlier genetic cross between HB3 (CQ-sensitive) and Dd2 (CQ-resistant) parasites (Wellems et al. 1990). Consistent with this, previous allelic exchange studies have unmasked the incompatibility of *pfcr* alleles with certain genetic backgrounds (Valderramos et al. 2010). As point mutations in the gene encoding the DV-resident *P. falciparum* multidrug resistance gene 1 (PfMDR1) transporter have previously been found to modulate *pfcr*-mediated CQR in some parasite strains (Sanchez et al. 2010), we speculate that *pfmdr1* may serve as a secondary genetic determinant of CQR evolution. It is conceivable that *pfmdr1* mutations might modulate the accessibility of *pfcr* mutational trajectories, akin to the recently documented capacity of the *GTP cyclohydrolase 1* (*gch1*) gene to enhance the accessibility of *pfdhfr* mutational trajectories in the evolution of pyrimethamine resistance (Kumpomsin et al. 2014). It remains to be determined whether PfMDR1 mutations S1034C and D1246Y (Mehlotra et al. 2008), present in 7G8 but not Ecu1110 parasites, might partly account for the different in vitro growth rates observed between parasites encoding identical (Ecu1110) *pfcr* alleles in these two genetic backgrounds. With the availability of validated genetic engineering strategies targeting both *pfmdr1* (Veiga et al., submitted) and *pfcr*, further exploration of the epistatic interactions between these two critical drug resistance loci is now possible.

In our analysis, the Ecu1110 PfCRT haplotype was identified as an accessible mutational precursor of the quintuple-SNP 7G8 haplotype, which was relatively more CQ-resistant and less deleterious to parasite growth. Our data support the rise of the 7G8 PfCRT haplotype in multiple geographical loci, where the Ecu1110-type haplotype has also been documented albeit at far lower frequencies (Nagesha et al. 2003; Vieira et al. 2004), as well as the ultimate success of the 7G8 PfCRT haplotype in spreading across vast tracts of the malaria-endemic world (Sa and Twu 2010). To date, 7G8 *pfcr* is at or near fixation in South America (Vieira et al. 2004; Griffing et al. 2010) and the Western Pacific (Koleala et al. 2015) and has been identified in some surveys of parasites from Africa, the Indian subcontinent, and Southeast Asia (Gama et al. 2010; Khattak et al. 2013; Chauhan et al. 2014; Tan et al. 2014). Notably, prior CQ and AQ use has been documented in each of these geographical regions, leading to the earlier conjecture that AQ might have driven the selection for 7G8 *pfcr* (Sa et al. 2009; Beshir et al. 2010). Considering interindividual variability in peak blood CQ concentration achieved in response to the standard CQ dose of 25 mg/kg (Ducharme and Farinotti 1996), the long terminal elimination half-life of CQ (Gustafsson et al. 1983), as well as the deployment of prophylactic chloroquinated and/or amodiaquinated salts (Payne 1988), we posit that the evolution of mutant *pfcr*

was likely facilitated by sustained subtherapeutic drug concentrations in these populations. It is notable that in our delineation of *pfcr*t mutational pathways, md-CQ, the active metabolite of CQ, was associated with a higher pathway predictive ability. A comparison of the pharmacology of CQ and md-CQ in the setting of the parasite DV will be essential to contextualizing these differences. To our knowledge, the accumulation of md-CQ in the parasite DV of CQ-resistant versus CQ-sensitive strains has yet to be explored.

Beyond CQR, our results also corroborate the pleiotropic role of PfCRT in modulating responses to critical first-line ACT component drugs and shed light on the opposing selective pressures exerted by these compounds. Notably, parasites encoding 7G8 *pfcr*t exhibited significant, high-level cross-resistance between CQ and md-AQ (the active metabolite of AQ), whereas their susceptibility to both AS and LUM was significantly increased as compared with wild-type *pfcr*t-expressing parasites. Accordingly, sole use of the ACT formulation AS–AQ in geographical regions where the 7G8 PfCRT haplotype is established should be avoided. A contributory role for AQ in facilitating *pfcr*t evolution of the drug-resistant Ecu1110 and 7G8 alleles is further supported by the shared subset of mutational trajectories that were favored by CQ and AQ in our analysis.

Our combinatorial evolutionary modeling sheds light on the capacity of *P. falciparum* parasites to produce and sustain very rare bursts of mutational events. In part due to selective pressures from one or more antimalarial agents acting upon an immutable host factor (e.g., heme), such mutational events were likely responsible for generating stably persisting drug-resistant *pfcr*t alleles that ultimately caused the global loss of CQ efficacy. Of particular concern is the recent emergence of artemisinin resistance in Southeast Asia, driven largely by point mutations in the *k13* gene that arose in genetically distinct parasite subpopulations (Miotto et al. 2013; Ariey et al. 2014; Straimer et al. 2015; Takala-Harrison et al. 2015). These clonal expansions of *k13*-mutant parasites suggest the selection of several favorable genetic backgrounds, resulting in population bottlenecks that might have facilitated parasite progression via fitness valleys (Miotto et al. 2015). Compounding this situation is the even more recent advent of piperazine resistance, which is now leading to treatment failures with the first-line regimen dihydroartemisinin–piperazine (Saunders et al. 2014; Duru et al. 2015; Amaratunga et al. 2016). The genetic basis of piperazine resistance is presently elusive, partly because of clonal subpopulation structures that hinder initial genome-wide association studies to pinpoint causal resistance determinants. Genetic and drug susceptibility profiling of newly resistant strains can also inform the selection of drug regimens that exert opposing selective pressures as a means to constrain the evolution of multidrug-resistant parasites. Given the central role of chemotherapy in alleviating the worldwide burden of malaria, leveraging genomic surveillance of malarial parasites with evolutionary and population genetic principles will facilitate detection of selection signatures that could compromise the efficacy of our present arsenal of antimalarial drugs.

Materials and Methods

Parasite Cultivation

Plasmodium falciparum–infected human erythrocytes were cultured at 4% hematocrit in 0.5% Albumax II (Invitrogen)–supplemented RPMI-1640 culture medium (Straimer et al. 2015) at 37 °C, 5% O₂/5% CO₂/90% N₂. Genetic modification of the parasite *pfcr*t locus is detailed in [supplementary methods, Supplementary Material online](#).

Drug Susceptibility Assays

To assess in vitro drug susceptibility, parasites were dispensed into 96-well plates containing a 2-fold dilution series of CQ ± 0.8 μM VP, md-CQ, md-AQ, LUM, or AS, prealiquoted with a BioTek Precision Pipetting System. Parasites were incubated at 2% final hematocrit in culture medium containing 50 mM HEPES (4-(2-hydroxyethyl)-1-piperazineethanesulfonic acid). After 72 h, parasites were stained with SYBR Green I and MitoTracker Deep Red, and growth was determined using an Accuri C6 flow cytometer (Ekland et al. 2011). Drug inhibitory concentrations that cause 50% (IC₅₀) or 90% (IC₉₀) inhibition of parasite growth were calculated as previously described (Valderramos et al. 2010). Reversibility of CQR by 0.8 μM VP is expressed as the CQ RMI, equivalent to the quotient of the CQ + VP IC₅₀ divided by the CQ IC₅₀ (Mehlotra et al. 2001). Statistical significance was determined via nonparametric Mann–Whitney *U* tests using GraphPad Prism 6 software.

In Vitro Growth Assays

In vitro fitness of recombinant and reference parasite lines was assessed in 1:1 coculture assays with the fluorescent reporter line NF54^{eGFP} (R^{GFP}). To generate R^{GFP}, a cassette encoding the enhanced GFP (eGFP) fluorescence probe flanked by 5′ hsp70 and 3′ hsp86 untranslated regions (UTRs) was genomically integrated into CQ-sensitive (wild-type *pfcr*t) NF54-*attB* parasites via *attB* × *attP*-based recombination catalyzed by the mycobacteriophage Bxb1 integrase (Adjalley et al. 2010). The robustness of this fluorescence reporter line was recently validated in vitro in fitness studies conducted in blood stage parasites (Baragana et al. 2015). Assays were initiated by preparing cocultures consisting of R^{GFP} (GFP⁺) and a single *pfcr*t-modified test line (GFP[−]) in a 1:1 ratio with respect to final parasitemia of each line. Using flow cytometric detection of eGFP, expressed by the reporter line, as well as the far-red fluorescent dye SYTO61, which facilitates differentiation between uninfected and infected red blood cells (Fu et al. 2010), the GFP[−] proportion of parasites was monitored for ten generations and used to derive the per-generation selection coefficient (*s*) for each test strain, as described in [Supplementary methods, Supplementary Material online](#). Statistical significance was assessed via two-way analysis of variance (ANOVA) with Sidak's post hoc test using GraphPad Prism 6 software.

Modeling of *pfcr*t Evolutionary Trajectories

In our mutational model, the total fitness associated with each *pfcr*t allele (*f_T*) was derived from the relationship $f_T = af_D + (1-a)f_C$, where *f_D* is the fitness index attributable to drug resistance, *f_C* is the fitness index attributable to parasite

growth in the absence of drug, and a is the drug pressure coefficient (range for each parameter: 0 to 1). The f_D index is equivalent to the IC_{50} value for a parasite line, normalized to the highest IC_{50} value observed among all combinatorial lines for a given drug. Similarly, the f_G index is equivalent to the relative in vitro growth (ω') of a parasite line in the absence of drug, normalized to the highest observed ω' value. Thus, in the case of full drug pressure ($a = 1$), the highest f_T value is ascribed to the *pfcr* allele that confers the highest degree of resistance, whereas in the completely drug-free environment ($a = 0$), the highest f_T value is shown by the *pfcr* allele that confers maximum parasite growth.

We adapted previously established methods (Lozovsky et al. 2009; Brown et al. 2010; Kumpornsin et al. 2014) to explore seven distinct mutational scenarios that lead to the evolution of Ecu1110 *pfcr* from the GC03 (wild-type) *pfcr* allele. These mutational scenarios are as follows: $0 \rightarrow 1 \rightarrow 2 \rightarrow 3 \rightarrow 4$; $0 \rightarrow 1 \rightarrow 2 \rightarrow 4$; $0 \rightarrow 1 \rightarrow 3 \rightarrow 4$; $0 \rightarrow 2 \rightarrow 3 \rightarrow 4$; $0 \rightarrow 1 \rightarrow 4$; $0 \rightarrow 2 \rightarrow 4$; and $0 \rightarrow 3 \rightarrow 4$, where each number corresponds to the number of total mutations acquired. For all hypothetical *pfcr* alleles comprising each mutational scenario, adaptive landscapes were generated by random sampling of f_D and f_G values from normal distributions based on *pfcr* allele-specific means and SEMs. To examine the role of drug pressure on mutational pathway accessibility, the drug pressure coefficient a was varied from 0 to 1, in increments of 0.1. We note that f_T and the experimentally derived growth selection coefficient s were in agreement ($R^2 = 0.974$) for growth experiments performed with 7.5 nM CQ ($a = 0.04$). Evolutionary excursions along each landscape were then simulated by randomly choosing one or more mutations, depending on the mutational scenario. The probability of a new mutant allele occurring is equal to the total fitness difference (Δf_T) between the new allele and the precursor allele. In our simulations, a uniform random number (r) was selected. The new allele was accepted only if $r < \Delta f_T$. A new mutant was only accepted if its f_T value was larger than that of its precursor allele. To calculate pathway probabilities, we simulated 10^4 normal-distributed adaptive landscapes and explored each with 10^5 independent iterations. The pathway probability was then calculated from the formula $P_i = N_i / N_{\text{total}}$, where P_i is the probability that parasites evolve along pathway i , N_i is the number of times that the simulations achieve the Ecu_{ABCD} allele by traversing pathway i , and N_{total} is the total number of runs ($N_{\text{total}} = 10^9$ in our analysis). All simulations were performed using MATLAB software.

Supplementary Material

Supplementary tables S1–S12, figures S1–S6, methods are available at *Molecular Biology and Evolution* online (<http://www.mbe.oxfordjournals.org/>).

Acknowledgments

This work was supported by the National Institutes of Health (R01 AI50234 and AI109023 to D.A.F. and F30 AI114070 to S.J.G.); the Office of Higher Education Commission and Mahidol University under the National Research

Universities Initiative (to T.C. and C.M.); and the Thailand Research Fund and Mahidol University (TRG5880157 to C.M. and RSA5880062 to T.C.).

References

- Adhin MR, Labadie-Bracho M, Bretas G. 2013. Molecular surveillance as monitoring tool for drug-resistant *Plasmodium falciparum* in Suriname. *Am J Trop Med Hyg.* 89:311–316.
- Adjalley SH, Lee MC, Fidock DA. 2010. A method for rapid genetic integration into *Plasmodium falciparum* utilizing mycobacteriophage Bxb1 integrase. *Methods Mol Biol.* 634:87–100.
- Amaratunga C, Lim P, Suon S, Sreng S, Mao S, Sopha C, Sam B, Dek D, Try V, Amato R, et al. 2016. Dihydroartemisinin-piperazine resistance in *Plasmodium falciparum* malaria in Cambodia: a multisite prospective cohort study. *Lancet Infect Dis.* doi: 10.1016/S1473-3099(15)00487-9.
- Amaratunga C, Sreng S, Mao S, Tullo GS, Anderson JM, Chuor CM, Suon S, Fairhurst RM. 2014. Chloroquine remains effective for treating *Plasmodium vivax* malaria in Pursat Province, Western Cambodia. *Antimicrob Agents Chemother.* 58:6270–6272.
- Ariey F, Witkowski B, Amaratunga C, Beghain J, Langlois AC, Khim N, Kim S, Duru V, Bouchier C, Ma L, et al. 2014. A molecular marker of artemisinin-resistant *Plasmodium falciparum* malaria. *Nature* 505:50–55.
- Baragana B, Hallyburton I, Lee MC, Norcross NR, Grimaldi R, Otto TD, Proto WR, Blagborough AM, Meister S, Wirjanata G, et al. 2015. A novel multiple-stage antimalarial agent that inhibits protein synthesis. *Nature* 522:315–320.
- Baro NK, Callaghan PS, Roepe PD. 2013. Function of resistance conferring *Plasmodium falciparum* chloroquine resistance transporter isoforms. *Biochemistry* 52:4242–4249.
- Beshir K, Sutherland CJ, Merinopoulos I, Durrani N, Leslie T, Rowland M, Hallett RL. 2010. Amodiaquine resistance in *Plasmodium falciparum* malaria in Afghanistan is associated with the *pfcr* SVMNT allele at codons 72 to 76. *Antimicrob Agents Chemother.* 54:3714–3716.
- Bopp SE, Manary MJ, Bright AT, Johnston GL, Dharia NV, Luna FL, McCormack S, Plouffe D, McNamara CW, Walker JR, et al. 2013. Mitotic evolution of *Plasmodium falciparum* shows a stable core genome but recombination in antigen families. *PLoS Genet.* 9:e1003293.
- Brown KM, Costanzo MS, Xu W, Roy S, Lozovsky ER, Hartl DL. 2010. Compensatory mutations restore fitness during the evolution of dihydrofolate reductase. *Mol Biol Evol.* 27:2682–2690.
- Brown TS, Jacob CG, Silva JC, Takala-Harrison S, Djimde A, Dondorp AM, Fukuda M, Noedl H, Nyunt MM, Kyaw MP, et al. 2015. *Plasmodium falciparum* field isolates from areas of repeated emergence of drug resistant malaria show no evidence of hypermutator phenotype. *Infect Genet Evol.* 30:318–322.
- Burkot TR, Williams JL, Schneider I. 1984. Infectivity to mosquitoes of *Plasmodium falciparum* clones grown in vitro from the same isolate. *Trans R Soc Trop Med Hyg.* 78:339–341.
- Callaghan PS, Hassett MR, Roepe PD. 2015. Functional comparison of 45 naturally occurring isoforms of the *Plasmodium falciparum* chloroquine resistance transporter (PfCRT). *Biochemistry* 54:5083–5094.
- Chauhan K, Pande V, Das A. 2014. DNA sequence polymorphisms of the *pfmdr1* gene and association of mutations with the *pfcr* gene in Indian *Plasmodium falciparum* isolates. *Infect Genet Evol.* 26:213–222.
- Chen N, Gao Q, Wang S, Wang G, Gatton M, Cheng Q. 2008. No genetic bottleneck in *Plasmodium falciparum* wild-type *pfcr* alleles re-emerging in Hainan Island, China, following high-level chloroquine resistance. *Antimicrob Agents Chemother.* 52:345–347.
- Claessens A, Hamilton WL, Kekre M, Otto TD, Faizullahoy A, Rayner JC, Kwiatkowski D. 2014. Generation of antigenic diversity in *Plasmodium falciparum* by structured rearrangement of *var* genes during mitosis. *PLoS Genet.* 10:e1004812.
- Combrinck JM, Mabothe TE, Ncokazi KK, Ambele MA, Taylor D, Smith PJ, Hoppe HC, Egan TJ. 2013. Insights into the role of heme in the mechanism of action of antimalarials. *ACS Chem Biol.* 8:133–137.

- Cooper RA, Hartwig CL, Ferdig MT. 2005. *pfprt* is more than the *Plasmodium falciparum* chloroquine resistance gene: a functional and evolutionary perspective. *Acta Trop.* 94:170–180.
- Costanzo MS, Brown KM, Hartl DL. 2011. Fitness trade-offs in the evolution of dihydrofolate reductase and drug resistance in *Plasmodium falciparum*. *PLoS One* 6:e19636.
- de Almeida A, Arez AP, Cravo PV, do Rosario VE. 2009. Analysis of genetic mutations associated with anti-malarial drug resistance in *Plasmodium falciparum* from the Democratic Republic of East Timor. *Malar J.* 8:59.
- de Koning-Ward TF, Gilson PR, Crabb BS. 2015. Advances in molecular genetic systems in malaria. *Nat Rev Microbiol.* 13:373–387.
- DePristo MA, Weinreich DM, Hartl DL. 2005. Missense meanderings in sequence space: a biophysical view of protein evolution. *Nat Rev Genet.* 6:678–687.
- Djimde A, Doumbo OK, Cortese JF, Kayentao K, Doumbo S, Diourte Y, Coulibaly D, Dicko A, Su XZ, Nomura T, et al. 2001. A molecular marker for chloroquine-resistant falciparum malaria. *N Engl J Med.* 344:257–263.
- Djimde AA, Doumbo OK, Traore O, Guindo AB, Kayentao K, Diourte Y, Niare-Doumbo S, Coulibaly D, Kone AK, Cissoko Y, et al. 2003. Clearance of drug-resistant parasites as a model for protective immunity in *Plasmodium falciparum* malaria. *Am J Trop Med Hyg.* 69:558–563.
- Ducharme J, Farinotti R. 1996. Clinical pharmacokinetics and metabolism of chloroquine. Focus on recent advancements. *Clin Pharmacokinet.* 31:257–274.
- Duru V, Khim N, Leang R, Kim S, Domergue A, Kloeung N, Ke S, Chy S, Eam R, Khean C, et al. 2015. *Plasmodium falciparum* dihydroartemisinin-piperazine failures in Cambodia are associated with mutant K13 parasites presenting high survival rates in novel piperazine in vitro assays: retrospective and prospective investigations. *BMC Med.* 13:305.
- Eastman RT, Dharia NV, Winzeler EA, Fidock DA. 2011. Piperazine resistance is associated with a copy number variation on chromosome 5 in drug-pressured *Plasmodium falciparum* parasites. *Antimicrob Agents Chemother.* 55:3908–3916.
- Eastman RT, Fidock DA. 2009. Artemisinin-based combination therapies: a vital tool in efforts to eliminate malaria. *Nat Rev Microbiol.* 7:864–874.
- Ecker A, Lakshmanan V, Sinnis P, Coppens I, Fidock DA. 2011. Evidence that mutant PfCRT facilitates the transmission to mosquitoes of chloroquine-treated *Plasmodium* gametocytes. *J Infect Dis.* 203:228–236.
- Ecker A, Lehane AM, Clain J, Fidock DA. 2012. PfCRT and its role in antimalarial drug resistance. *Trends Parasitol.* 28:504–514.
- Egan TJ, Kuter D. 2013. Dual-functioning antimalarials that inhibit the chloroquine-resistance transporter. *Future Microbiol.* 8:475–489.
- Ekland EH, Schneider J, Fidock DA. 2011. Identifying apicoplast-targeting antimalarials using high-throughput compatible approaches. *FASEB J.* 25:3583–3593.
- Fidock DA, Nomura T, Talley AK, Cooper RA, Dzekunov SM, Ferdig MT, Ursos LM, Sidhu AB, Naude B, Deitsch KW, et al. 2000. Mutations in the *P. falciparum* digestive vacuole transmembrane protein PfCRT and evidence for their role in chloroquine resistance. *Mol Cell.* 6:861–871.
- Fitch CD. 2004. Ferriprotoporphyrin IX, phospholipids, and the antimalarial actions of quinoline drugs. *Life Sci.* 74:1957–1972.
- Fu Y, Tilley L, Kenny S, Klionis N. 2010. Dual labeling with a far red probe permits analysis of growth and oxidative stress in *P. falciparum*-infected erythrocytes. *Cytometry A* 77:253–263.
- Gama BE, de Oliveira NK, Zalis MG, de Souza JM, Santos F, Daniel-Ribeiro CT, Ferreira-da-Cruz Mde F. 2009. Chloroquine and sulphadoxine-pyrimethamine sensitivity of *Plasmodium falciparum* parasites in a Brazilian endemic area. *Malar J.* 8:156.
- Gama BE, Pereira-Carvalho GA, Lutucuta Kosi FJ, Almeida de Oliveira NK, Fortes F, Rosenthal PJ, Daniel-Ribeiro CT, de Fatima Ferreira-da-Cruz M. 2010. *Plasmodium falciparum* isolates from Angola show the StctVMNT haplotype in the *pfprt* gene. *Malar J.* 9:174.
- Goswami D, Dhiman S, Rabha B, Kumar D, Baruah I, Sharma DK, Veer V. 2014. PfCRT mutant haplotypes may not correspond with chloroquine resistance. *J Infect Dev Ctries.* 8:768–773.
- Griffing S, Syphard L, Sridaran S, McCollum AM, Mixson-Hayden T, Vinayak S, Villegas L, Barnwell JW, Escalante AA, Udhayakumar V. 2010. *pfmdr1* amplification and fixation of *pfprt* chloroquine resistance alleles in *Plasmodium falciparum* in Venezuela. *Antimicrob Agents Chemother.* 54:1572–1579.
- Gustafsson LL, Walker O, Alvan G, Beerhmann B, Estevez F, Gleisner L, Lindstrom B, Sjoqvist F. 1983. Disposition of chloroquine in man after single intravenous and oral doses. *Br J Clin Pharmacol.* 15:471–479.
- Hartl DL. 2014. What can we learn from fitness landscapes? *Curr Opin Microbiol.* 21:51–57.
- Hastings IM, Bray PG, Ward SA. 2002. Parasitology. A requiem for chloroquine. *Science* 298:74–75.
- Hawley SR, Bray PG, Mungthin M, Atkinson JD, O'Neill PM, Ward SA. 1998. Relationship between antimalarial drug activity, accumulation, and inhibition of heme polymerization in *Plasmodium falciparum* in vitro. *Antimicrob Agents Chemother.* 42:682–686.
- Henriques G, Hallett RL, Beshir KB, Gadalla NB, Johnson RE, Burrow R, van Schalkwyk DA, Sawa P, Omar SA, Clark TG, et al. 2014. Directional selection at the *pfmdr1*, *pfprt*, *pfubp1* and *pfap2mu* loci of *Plasmodium falciparum* in Kenyan children treated with ACT. *J Infect Dis.* 210:2001–2008.
- Hughes D, Andersson DI. 2015. Evolutionary consequences of drug resistance: shared principles across diverse targets and organisms. *Nat Rev Genet.* 16:459–471.
- Jiang PP, Corbett-Detig RB, Hartl DL, Lozovsky ER. 2013. Accessible mutational trajectories for the evolution of pyrimethamine resistance in the malaria parasite *Plasmodium vivax*. *J Mol Evol.* 77:81–91.
- Johnson DJ, Fidock DA, Mungthin M, Lakshmanan V, Sidhu AB, Bray PG, Ward SA. 2004. Evidence for a central role for PfCRT in conferring *Plasmodium falciparum* resistance to diverse antimalarial agents. *Mol Cell.* 15:867–877.
- Khattak AA, Venkatesan M, Jacob CG, Artimovich EM, Nadeem MF, Nighat F, Hombhanje F, Mita T, Malik SA, Plowe CV. 2013. A comprehensive survey of polymorphisms conferring anti-malarial resistance in *Plasmodium falciparum* across Pakistan. *Malar J.* 12:300.
- Kogenaru M, de Vos MG, Tans SJ. 2009. Revealing evolutionary pathways by fitness landscape reconstruction. *Crit Rev Biochem Mol Biol.* 44:169–174.
- Koleala T, Karl S, Laman M, Moore BR, Benjamin J, Barnadas C, Robinson LJ, Kattenberg JH, Javati S, Wong R, et al. 2015. Temporal changes in *Plasmodium falciparum* anti-malarial drug sensitivity in vitro and resistance-associated genetic mutations in isolates from Papua New Guinea. *Malar J.* 14:37.
- Kumpornsini K, Modchang C, Heinberg A, Ekland EH, Jirawatcharadech P, Chobson P, Suwanakitti N, Chaotheing S, Wilairat P, Deitsch KW, et al. 2014. Origin of robustness in generating drug-resistant malaria parasites. *Mol Biol Evol.* 31:1649–1660.
- Lakshmanan V, Bray PG, Verdier-Pinard D, Johnson DJ, Horrocks P, Muhle RA, Alakpa GE, Hughes RH, Ward SA, Krogstad DJ, et al. 2005. A critical role for PfCRT K76T in *Plasmodium falciparum* verapamil-reversible chloroquine resistance. *EMBO J.* 24:2294–2305.
- Laufer MK, Takala-Harrison S, Dzinjalama FK, Stine OC, Taylor TE, Plowe CV. 2010. Return of chloroquine-susceptible falciparum malaria in Malawi was a reexpansion of diverse susceptible parasites. *J Infect Dis.* 202:801–808.
- Lewis IA, Wacker M, Olszewski KL, Cobbold SA, Baska KS, Tan A, Ferdig MT, Llinas M. 2014. Metabolic QTL analysis links chloroquine resistance in *Plasmodium falciparum* to impaired hemoglobin catabolism. *PLoS Genet.* 10:e1004085.
- Lozovsky ER, Chookajorn T, Brown KM, Imwong M, Shaw PJ, Kamchonwongpaisan S, Neafsey DE, Weinreich DM, Hartl DL. 2009. Stepwise acquisition of pyrimethamine resistance in the malaria parasite. *Proc Natl Acad Sci U S A.* 106:12025–12030.
- Mackinnon MJ, Marsh K. 2010. The selection landscape of malaria parasites. *Science* 328:866–871.

- Mallick PK, Joshi H, Valecha N, Sharma SK, Eapen A, Bhatt RM, Srivastava HC, Sutton PL, Dash AP, Bhasin VK. 2012. Mutant *pfprt* "SVMNT" haplotype and wild type *pfmdr1* "N86" are endemic in *Plasmodium vivax* dominated areas of India under high chloroquine exposure. *Malar J.* 11:16.
- Mehlotra RK, Fujioka H, Roepe PD, Janneh O, Ursos LM, Jacobs-Lorena V, McNamara DT, Bockarie MJ, Kazura JW, Kyle DE, et al. 2001. Evolution of a unique *Plasmodium falciparum* chloroquine-resistance phenotype in association with *pfprt* polymorphism in Papua New Guinea and South America. *Proc Natl Acad Sci U S A.* 98:12689–12694.
- Mehlotra RK, Matterna G, Bockarie MJ, Maguire JD, Baird JK, Sharma YD, Alifrangis M, Dorsey G, Rosenthal PJ, Fryauff DJ, et al. 2008. Discordant patterns of genetic variation at two chloroquine resistance loci in worldwide populations of the malaria parasite *Plasmodium falciparum*. *Antimicrob Agents Chemother.* 52:2212–2222.
- Mekonnen SK, Aseffa A, Berhe N, Teklehaymanot T, Clouse RM, Gebru T, Medhin G, Velavan TP. 2014. Return of chloroquine-sensitive *Plasmodium falciparum* parasites and emergence of chloroquine-resistant *Plasmodium vivax* in Ethiopia. *Malar J.* 13:244.
- Mharakurwa S, Sialumano M, Liu K, Scott A, Thuma P. 2013. Selection for chloroquine-sensitive *Plasmodium falciparum* by wild *Anopheles arabiensis* in Southern Zambia. *Malar J.* 12:453.
- Miotto O, Almagro-Garcia J, Manske M, Macinnis B, Campino S, Rockett KA, Amaratunga C, Lim P, Suon S, Sreng S, et al. 2013. Multiple populations of artemisinin-resistant *Plasmodium falciparum* in Cambodia. *Nat Genet.* 45:648–655.
- Miotto O, Amato R, Ashley EA, Maclnnis B, Almagro-Garcia J, Amaratunga C, Lim P, Mead D, Oyola SO, Dhorda M, et al. 2015. Genetic architecture of artemisinin-resistant *Plasmodium falciparum*. *Nat Genet.* 47:226–234.
- Mwai L, Ochong E, Abdirahman A, Kiara SM, Ward S, Kokwaro G, Sasi P, Marsh K, Borrmann S, Mackinnon M, et al. 2009. Chloroquine resistance before and after its withdrawal in Kenya. *Malar J.* 8:106.
- Nagesha HS, Casey GJ, Rieckmann KH, Fryauff DJ, Laksana BS, Reeder JC, Maguire JD, Baird JK. 2003. New haplotypes of the *Plasmodium falciparum* chloroquine resistance transporter (*pfprt*) gene among chloroquine-resistant parasite isolates. *Am J Trop Med Hyg.* 68:398–402.
- Okech BA, Existe A, Romain JR, Memnon G, Victor YS, de Rochars MB, Fukuda M. 2015. Therapeutic efficacy of chloroquine for the treatment of uncomplicated *Plasmodium falciparum* in Haiti after many decades of its use. *Am J Trop Med Hyg.* 92:541–545.
- Olson-Manning CF, Wagner MR, Mitchell-Olds T. 2012. Adaptive evolution: evaluating empirical support for theoretical predictions. *Nat Rev Genet.* 13:867–877.
- Ord R, Alexander N, Dunyo S, Hallett R, Jawara M, Targett G, Drakeley CJ, Sutherland CJ. 2007. Seasonal carriage of *pfprt* and *pfmdr1* alleles in Gambian *Plasmodium falciparum* imply reduced fitness of chloroquine-resistant parasites. *J Infect Dis.* 196:1613–1619.
- Palmer AC, Toprak E, Baym M, Kim S, Veres A, Bershtein S, Kishony R. 2015. Delayed commitment to evolutionary fate in antibiotic resistance fitness landscapes. *Nat Commun.* 6:7385.
- Park DJ, Lukens AK, Neafsey DE, Schaffner SF, Chang HH, Valim C, Ribacke U, Van Tyne D, Galinsky K, Galligan M, et al. 2012. Sequence-based association and selection scans identify drug resistance loci in the *Plasmodium falciparum* malaria parasite. *Proc Natl Acad Sci U S A.* 109:13052–13057.
- Patel JJ, Thacker D, Tan JC, Pleeter P, Checkley L, Gonzales JM, Deng B, Roepe PD, Cooper RA, Ferdig MT. 2010. Chloroquine susceptibility and reversibility in a *Plasmodium falciparum* genetic cross. *Mol Microbiol.* 78:770–787.
- Payne D. 1988. Did medicated salt hasten the spread of chloroquine resistance in *Plasmodium falciparum*? *Parasitol Today.* 4:112–115.
- Pelleau S, Moss EL, Dhingra SK, Volney B, Casteras J, Gabryszewski SJ, Volkman SK, Wirth DF, Legrand E, Fidock DA, et al. 2015. Adaptive evolution of malaria parasites in French Guiana: reversal of chloroquine resistance by acquisition of a mutation in *pfprt*. *Proc Natl Acad Sci U S A.* 112:11672–11677.
- Petersen I, Gabryszewski SJ, Johnston GL, Dhingra SK, Ecker A, Lewis RE, de Almeida MJ, Straimer J, Henrich PP, Palatulan E, et al. 2015. Balancing drug resistance and growth rates via compensatory mutations in the *Plasmodium falciparum* chloroquine resistance transporter. *Mol Microbiol.* 97:381–395.
- Poelwijk FJ, Kiviet DJ, Weinreich DM, Tans SJ. 2007. Empirical fitness landscapes reveal accessible evolutionary paths. *Nature* 445:383–386.
- Roepe PD. 2009. Molecular and physiologic basis of quinoline drug resistance in *Plasmodium falciparum* malaria. *Future Microbiol.* 4:441–455.
- Roepe PD. 2011. PfCRT-mediated drug transport in malarial parasites. *Biochemistry* 50:163–171.
- Rosenthal PJ. 2013. The interplay between drug resistance and fitness in malaria parasites. *Mol Microbiol.* 89:1025–1038.
- Sa JM, Twu O. 2010. Protecting the malaria drug arsenal: halting the rise and spread of amodiaquine resistance by monitoring the PfCRT SVMNT type. *Malar J.* 9:374.
- Sa JM, Twu O, Hayton K, Reyes S, Fay MP, Ringwald P, Wellems TE. 2009. Geographic patterns of *Plasmodium falciparum* drug resistance distinguished by differential responses to amodiaquine and chloroquine. *Proc Natl Acad Sci U S A.* 106:18883–18889.
- Sanchez CP, Dave A, Stein WD, Lanzer M. 2010. Transporters as mediators of drug resistance in *Plasmodium falciparum*. *Int J Parasitol.* 40:1109–1118.
- Saunders DL, Vanachayangkul P, Lon C, U.S. Army Military Malaria Research Program, National Center for Parasitology, Entomology, and Malaria Control (CNM), Royal Cambodian Armed Forces. 2014. Dihydroartemisinin-piperazine failure in Cambodia. *N Engl J Med.* 371:484–485.
- Sidhu AB, Verdier-Pinard D, Fidock DA. 2002. Chloroquine resistance in *Plasmodium falciparum* malaria parasites conferred by *pfprt* mutations. *Science* 298:210–213.
- Sisowath C, Petersen I, Veiga MI, Martensson A, Premji Z, Bjorkman A, Fidock DA, Gil JP. 2009. *In vivo* selection of *Plasmodium falciparum* parasites carrying the chloroquine-susceptible *pfprt* K76 allele after treatment with artemether-lumefantrine in Africa. *J Infect Dis.* 199:750–757.
- Straimer J, Gnadig NF, Witkowski B, Amaratunga C, Duru V, Ramadani AP, Dacheux M, Khim N, Zhang L, Lam S, et al. 2015. K13-propeller mutations confer artemisinin resistance in *Plasmodium falciparum* clinical isolates. *Science* 347:428–431.
- Straimer J, Lee MC, Lee AH, Zeitler B, Williams AE, Pearl JR, Zhang L, Rebar EJ, Gregory PD, Llinas M, et al. 2012. Site-specific genome editing in *Plasmodium falciparum* using engineered zinc-finger nucleases. *Nat Methods.* 9:993–998.
- Su X, Kirkman LA, Fujioka H, Wellems TE. 1997. Complex polymorphisms in an approximately 330 kDa protein are linked to chloroquine-resistant *P. falciparum* in Southeast Asia and Africa. *Cell* 91:593–603.
- Summers RL, Dave A, Dolstra TJ, Bellanca S, Marchetti RV, Nash MN, Richards SN, Goh V, Schenk RL, Stein WD, et al. 2014. Diverse mutational pathways converge on saturable chloroquine transport via the malaria parasite's chloroquine resistance transporter. *Proc Natl Acad Sci U S A.* 111:E1759–E1767.
- Summers RL, Nash MN, Martin RE. 2012. Know your enemy: understanding the role of PfCRT in drug resistance could lead to new antimalarial tactics. *Cell Mol Life Sci.* 69:1967–1995.
- Takala-Harrison S, Jacob CG, Arze C, Cummings MP, Silva JC, Dondorp AM, Fukuda MM, Hien TT, Mayxay M, Noedl H, et al. 2015. Independent emergence of artemisinin resistance mutations among *Plasmodium falciparum* in Southeast Asia. *J Infect Dis.* 211:670–679.
- Tan LL, Lau TY, Timothy W, Prabakaran D. 2014. Full-length sequence analysis of chloroquine resistance transporter gene in *Plasmodium falciparum* isolates from Sabah, Malaysia. *Scientific World J.* 2014:935846.
- Trape JF. 2001. The public health impact of chloroquine resistance in Africa. *Am J Trop Med Hyg.* 64:12–17.

- Tukwasibwe S, Mugenyi L, Mbogo GW, Nankoberanyi S, Maiteki-Sebuguzi C, Joloba ML, Nsobyia SL, Staedke SG, Rosenthal PJ. 2014. Differential prevalence of transporter polymorphisms in symptomatic and asymptomatic falciparum malaria infections in Uganda. *J Infect Dis.* 210:154–157.
- Valderramos SG, Valderramos JC, Musset L, Purcell LA, Mercereau-Puijalon O, Legrand E, Fidock DA. 2010. Identification of a mutant PfCRT-mediated chloroquine tolerance phenotype in *Plasmodium falciparum*. *PLoS Pathog.* 6:e1000887.
- Venkatesan M, Gadalla NB, Stepniewska K, Dahal P, Nsanzabana C, Moriera C, Price RN, Martensson A, Rosenthal PJ, Dorsey G, et al. 2014. Polymorphisms in *Plasmodium falciparum* chloroquine resistance transporter and multidrug resistance 1 genes: parasite risk factors that affect treatment outcomes for *P. falciparum* malaria after artemether-lumefantrine and artesunate-amodiaquine. *Am J Trop Med Hyg.* 91:833–843.
- Vieira PP, Ferreira MU, Alecrim M, Alecrim WD, da Silva LH, Sihuincha MM, Joy DA, Mu J, Su XZ, Zalis MG. 2004. *pfcr*t polymorphism and the spread of chloroquine resistance in *Plasmodium falciparum* populations across the Amazon Basin. *J Infect Dis.* 190:417–424.
- Waller KL, Muhle RA, Ursos LM, Horrocks P, Verdier-Pinard D, Sidhu AB, Fujioka H, Roepe PD, Fidock DA. 2003. Chloroquine resistance modulated in vitro by expression levels of the *Plasmodium falciparum* chloroquine resistance transporter. *J Biol Chem.* 278:33593–33601.
- Wang X, Mu J, Li G, Chen P, Guo X, Fu L, Chen L, Su X, Welles TE. 2005. Decreased prevalence of the *Plasmodium falciparum* chloroquine resistance transporter 76T marker associated with cessation of chloroquine use against *P. falciparum* malaria in Hainan, People's Republic of China. *Am J Trop Med Hyg.* 72:410–414.
- Weinreich DM, Delaney NF, Depristo MA, Hartl DL. 2006. Darwinian evolution can follow only very few mutational paths to fitter proteins. *Science* 312:111–114.
- Wellems TE. 2002. *Plasmodium* chloroquine resistance and the search for a replacement antimalarial drug. *Science* 298:124–126.
- Wellems TE. 2004. Transporter of a malaria catastrophe. *Nat Med.* 10:1169–1171.
- Wellems TE, Panton LJ, Gluzman IY, do Rosario VE, Gwadz RW, Walker-Jonah A, Krogstad DJ. 1990. Chloroquine resistance not linked to *mdr*-like genes in a *Plasmodium falciparum* cross. *Nature* 345:253–255.
- White NJ. 2008. Qinghaosu (artemisinin): the price of success. *Science* 320:330–334.
- White NJ, Pukrittayakamee S, Hien TT, Faiz MA, Mokuolu OA, Dondorp AM. 2014. Malaria. *Lancet* 383:723–735.
- Wongsrichanalai C, Pickard AL, Wernsdorfer WH, Meshnick SR. 2002. Epidemiology of drug-resistant malaria. *Lancet Infect Dis.* 2:209–218.
- Wootton JC, Feng X, Ferdig MT, Cooper RA, Mu J, Baruch DI, Magill AJ, Su XZ. 2002. Genetic diversity and chloroquine selective sweeps in *Plasmodium falciparum*. *Nature* 418:320–323.
- Wu EY, Walsh AR, Materne EC, Hiltner EP, Zielinski B, Miller BR 3rd, Mawby L, Modeste E, Parish CA, Barnes WM, et al. 2015. A conservative isoleucine to leucine mutation causes major rearrangements and cold sensitivity in KlenTaq1 DNA polymerase. *Biochemistry* 54:881–889.
- Zheng Q. 2003. Mathematical issues arising from the directed mutation controversy. *Genetics* 164:373–379.